Published July 7, 2016

ORIGINAL RESEARCH

A Consensus Map in Cultivated Hexaploid Oat Reveals Conserved Grass Synteny with Substantial Subgenome Rearrangement

Ashley S. Chaffin,† Yung-Fen Huang,† Scott Smith,† Wubishet A. Bekele, Ebrahiem Babiker, Belaghihalli N. Gnanesh, Bradley J. Foresman, Steven G. Blanchard, Jeremy J. Jay, Robert W. Reid, Charlene P. Wight, Shiaoman Chao, Rebekah Oliver, Emir Islamovic, Frederic L. Kolb, Curt McCartney, Jennifer W. Mitchell Fetch, Aaron D. Beattie, Åsmund Bjørnstad, J. Michael Bonman, Tim Langdon, Catherine J. Howarth, Cory R. Brouwer, Eric N. Jellen, Kathy Esvelt Klos, Jesse A. Poland, Tzung-Fu Hsieh, Ryan Brown, Eric Jackson, Jessica A. Schlueter* and Nicholas A. Tinker*

Abstract

Hexaploid oat (*Avena sativa* L., 2*n* = 6*x* = 42) is a member of the Poaceae family and has a large genome (~12.5 Gb) containing 21 chromosome pairs from three ancestral genomes. Physical rearrangements among parental genomes have hindered the development of linkage maps in this species. The objective of this work was to develop a single high-density consensus linkage map that is representative of the majority of commonly grown oat varieties. Data from a cDNA-derived single-nucleotide polymorphism (SNP) array and genotyping-by-sequencing (GBS) were collected from the progeny of 12 biparental recombinant inbred line populations derived from 19 parents representing oat germplasm cultivated primarily in North America. Linkage groups from all mapping populations were compared to identify 21 clusters of conserved collinearity. Linkage groups within each cluster were then merged into 21 consensus chromosomes, generating a framework consensus map of 7202 markers spanning 2843 cM. An additional 9678 markers were placed on this map with a lower degree of certainty. Assignment to physical chromosomes with high confidence was made for nine chromosomes. Comparison of homeologous regions among oat chromosomes and matches to orthologous regions of rice (*Oryza sativa* L.) reveal that the hexaploid oat genome has been highly rearranged relative to its ancestral diploid genomes as a result of frequent translocations among chromosomes. Heterogeneous chromosome rearrangements among populations were also evident, probably accounting for the failure of some linkage groups to match the consensus. This work contributes to a further understanding of the organization and evolution of hexaploid grass genomes.

Core Ideas

- We constructed a hexaploid oat consensus map from 12 populations representing 19 parents.
- The map represents the most common physical chromosome arrangements in oat.
- Deviations from the consensus map may indicate physical rearrangements.
- Large chromosomal translocations vary among different varieties.
- There is regional synteny with rice but considerable subgenome rearrangement.

A.S. Chaffin, S.G. Blanchard, J.J. Jay, R.W. Reid, C.R. Brouwer, J.A. Schlueter, Dep. Bioinformatics and Genomics, Univ. North Carolina at Charlotte, 9201 University City Blvd, Charlotte, NC 28223; Y.-F. Huang, W.A. Bekele, C.P. Wight, N.A. Tinker, Ottawa Research and Development Centre, Agriculture and Agri-Food Canada, 960 Carling Ave, CE Farm, KW Neatby Bldg, Ottawa, ON K1A 0C6, Canada; Y.-F. Huang, Department of Agronomy, National Taiwan University, No. 1, Section 4, Roosevelt Road, Taipei 106, Taiwan; S. Smith, T.-F. Hsieh, Dep. Plant and Microbial Biology, North Carolina State Univ., 600 Laureate Way, Raleigh, NC 27695 and Plants for Human Health Institute, North Carolina State Univ., Kannapolis, NC 28081; E. Babiker, E. Islamovic, J.M. Bonman, K. Esvelt Klos, Small Grains and Potato Germplasm Research Unit, USDA-ARS, 1691 S 2700 W, Aberdeen, ID 83210; B.N. Gnanesh, Dep. Plant Sci., Univ. Manitoba, 66 Dafoe Road, Winnipeg, MB R3T 2N2, Canada; B.N. Gnanesh, C. McCartney, Agriculture and Agri-Food Canada, 101 Route 100, Morden, MB, R6M 1Y5, Canada; B.J. Foresman, F.L. Kolb, Dep. Crop Sciences, 1102 South Goodwin Ave, Univ. Illinois, Urbana, IL 61801; S.G. Blanchard, J.J. Jay, R.W. Reid, C.R. Brouwer, Bioinformatics Services Division, Univ. North Carolina at Charlotte, 150 N Research Campus Dr, Kannapolis, NC 28081; S. Chao, Cereal Crops Research, USDA-ARS, 1605 Albrecht Blvd N, Fargo, ND 58102; R. Oliver, Dep. Plant Sciences, PO Box 6050, North Dakota State University, Fargo, ND 58108; E. Islamovic, BASF Plant Science LP, 26 Davis Dr, Research Triangle Park, NC 27709; J.W. Mitchell Fetch, Agriculture and Agri-Food Canada, 2701 Grand Valley Road, Brandon, MB R7A 5Y3, Canada; A.D.

Published in Plant Genome
Volume 9. doi: 10.3835/plantgenome2015.10.0102

Beattie, Dep. Plant Sciences, 51 Campus Drive, Univ. Saskatchewan, Saskatoon, SK S7N 5A8, Canada; Å. Bjørnstad, Dep. Plant and Environmental Sciences, PO Box 5003, Norwegian Univ. Life Sciences, N-1432 Ås, Norway; T. Langdon, C.J. Howarth, Inst. Biological, Environmental and Rural Sciences, Aberystwyth University, Gogerddan, Aberystwyth, Ceredigion SY23 3EE, UK; E.N. Jellen, Dep. Plant and Wildlife Sciences, 5009 LSB, Brigham Young Univ., Provo, UT 84602; J.A. Poland, Wheat Genetics Resource Center, Dep. Plant Pathology and Dep. Agronomy, 4024 Throckmorton Plant Sciences Center, Kansas State Univ., Manhattan, KS 66506; R.Brown, United States Patent and Trademark Office, 400 Dulany Street, Alexandria, VA 22314; E. Jackson, General Mills Crop Sciences, 1990 Kimball Ave, Manhattan, KS 66506. † A.S. Chaffin, Y.-F. Huang, and S. Smith contributed equally to this work. Received 21 Oct. 2015. Accepted 23 Jan. 2016. *Corresponding authors (jschluet@uncc.edu; nick.tinker@agr.gc.ca).

Abbreviations: BLASTn, nucleotide basic local alignment search tool; GBS, Genotyping-by-sequencing; LD, linkage disequilibrium; MHP, monosomic hybrid plant; *rf*, recombination fraction; Mrg, merge, used to designate linkage groups that are the consensus of the underlying component maps primary consensus chromosome representation; SMUSH, Smooth Map Unitization by Slope Heuristics; SNP, single nucleotide polymorphisms.

THE GENUS *Avena* contains approximately 30 species, ranging in ploidy from diploid to hexaploid, with a base haploid chromosome number of seven. Of these, the hexaploid species *A. sativa* (oat), with a genome constitution of AACCDD, is the most studied and commercially important. Oat is produced worldwide as a food grain, feed grain, and fodder. It is also used as a high-quality starch base for cosmetics and skin care, and for the isolation of health-promoting nutraceutical compounds, including avenanthramides and β-glucans. Although oat is a minor crop compared with crops such as corn (*Zea mays* L.), wheat (*Triticum aestivum* L.), and rice, it is a major crop in many northern countries such as Canada, Russia, and the Scandinavian nations and it is produced in many other countries on a scale large enough that it can be considered a global crop. Worldwide production of oat grain is estimated to be 23 Mt per year (FAO, 2013).

Efforts to build genomics platforms in oat have often been challenging, because oat has a large, highly repetitive genome, estimated to have a haploid size of 12.5 Gbp (Yan et al., 2016). Although the oat genome is allohexaploid, with primarily disomic pairing, nonhomologous pairing is common. There are two documented major translocations, one involving the chromosomes designated as 7C and 17A (Jellen et al., 1994) and the other involving chromosomes 3C and 14D (Jellen et al., 1997). The 3C–14D translocation was originally reported in some plants of the 'Sun II' genetic background; it has since been observed in some other oat cultivars descended from the German landrace 'Markische Landsorte' (Jellen, unpublished data, 2012). For the 7C–17A rearrangement, the nontranslocated chromosomes appear mostly in the *A. sativa* ssp. *byzantina* (red oat) types and the translocated chromosomes appear frequently in the non-*byzantina* types (Jellen and Beard, 2000); however, breeders have commonly intercrossed these two germplasm pools. The absence of the translocation in the cultivar Kanota and its presence in the cultivar Ogle affected the ability to map the translocated chromosomes in a Kanota × Ogle population (O'Donoughue et al., 1995; Wight et al., 2003; Tinker et al., 2009). Maps of crosses made using parents with the diploid A genome (O'Donoughue et al., 1992; Kremer et al., 2001) were constructed to assist with mapping and understanding the more complex hexaploid genome. These diploid oat maps have been valuable in identifying the phylogenetic relationship of oat to other grass genomes (Gale and Devos, 1998). However, it has since become apparent that hexaploid oat chromosomes contain substantial rearrangements relative to the basic diploid ancestral chromosomes (Wight et al., 2003; Gutierrez-Gonzalez and Garvin, 2011). This may be caused by a high degree of similarity between the A and D genomes and/or the ability of the hexaploid to buffer and maintain substantial chromosome rearrangements.

Consensus-based linkage maps provide frameworks for ordered genes and genetic markers that are fundamentally important for many other scientific and applied genomic endeavors. Applications of consensus maps include inter- and intra-species genome comparisons, association mapping, molecular breeding, genetic diversity analysis, genome sequencing, and map-based cloning. A consensus linkage map is developed by merging and averaging a set of component maps made in segregating parental populations that are representative of a species. This is done to improve the estimation of marker order and intermarker distances and to average this information where differences exist. Importantly, it is also done because every component map contains a limited subset of segregating markers, and only by merging these can a more complete map be developed. A high-density consensus map containing sequence-based markers is a key tool in the development of a complete genome sequence because it provides a framework that can be used to order and orient contiguous DNA assemblies (contigs) and generate a usable pseudomolecule. Such a framework would be especially important in the assembly of the hexaploid oat genome, because it would provide the basis for differentiating and assigning positions to highly similar homeologous assemblies.

The first oat consensus map was based on a set of 985 SNPs assayed in 390 recombinant inbred lines from six biparental populations (Oliver et al., 2013). Since then, the SNP marker platform has been substantially improved (Tinker et al., 2014) and has been supplemented by high-density SNPs discovered through GBS (Tinker et al., 2014). In assessing the requirement for a new oat consensus map, we considered not only the increased availability of genetic markers in a larger number of segregating populations, but also the potential to correct errors in the previous map and the potential to better understand biological deviations among maps. Population-specific linkage maps often differ from a consensus map in marker order and intermarker distance for

reasons beyond statistical error. Recombination distance and gene orders can differ among accessions within a species, and oat may contain a substantial number of undocumented chromosomal rearrangements. Jellen and Beard (2000) reported that, in comparison to *A. sativa* ssp. *byzantina* accessions, 97% (77 out of 79) of *A. sativa* accessions possessed a translocated segment. Minor differences in marker order may not register on the scale of a linkage map but large-scale differences such as insertions, deletions, and translocations could have a profound effect on the establishment of a 'correct' or 'most representative' consensus map. By including a larger set of component maps from a set of target germplasm in the construction of a consensus, it may be possible to define a map that is representative of that germplasm sample. This consensus could then provide a baseline for further characterization of germplasm-specific rearrangements.

An additional goal of the previous oat consensus map was to reconcile the nomenclature of mapped chromosomes with the established cytogenetic nomenclature described by Sanz et al. (2010), which identified all 21 hexaploid oat chromosomes, assigned these to three subgenomes (A, D, and C), and identified putative intergenomic chromosome translocations. Oliver et al. (2013) used a strategy described by Fox et al. (2001), where known monosomic chromosome stocks in Sun II and Kanota were crossed with disomic stocks of Ogle or the cultivar 'TAM O-301' to produce a series of F_1 monosomic hybrid plants (MHPs). They then used 45 MHPs to anchor 15 of the 21 consensus chromosomes to physical chromosomes. The remaining chromosomes showed some heterogeneity in their anchor positions, but were anchored on the basis of the majority of the markers and/or an accompanying dilution analysis using Diversity Array Technology markers (DArT) (Jaccoud et al., 2001).

With the development of mature versions of new marker technologies for oat (Tinker et al., 2014) and with an increasing user base for these technologies, needs and opportunities arose to re-evaluate the consensus oat linkage map. In preliminary work, it became apparent that there was now ambiguity in the assignment of some chromosomes based on monosomic hybrids, and that there was some uncertainty regarding whether the existing map best represented the majority of new component maps. It was considered important to reassess the consensus map using a much larger set of markers and mapping progeny to provide the oat community with a more accurate and representative framework for applications in genome-wide association analysis, comparative genomics, and gene cloning. With these objectives came an increased awareness of the differences in genome organization among hexaploid oat parents and between wild and cultivated oat species. Therefore, it is our hope that the new consensus map will provide the best possible baseline from which new work on sequence-level comparative mapping can be further explored, and by which hexaploid oat can serve as a better model for hexaploid evolution in the grass family.

MATERIALS AND METHODS

Genetic Material and DNA Isolation

Genetic material used in this study, listed in Table 1 with the two-letter code used for each cross, included 12 biparental recombinant inbred line populations based on a total of 19 different inbred parents. An additional six MHP stocks were developed as described by Oliver et al. (2013) and added to the 45 MHPs previously studied. DNA isolation was performed using a variety of methods, as some samples were available from previous studies. The preparation of DNA stocks from the CH, HZ, OT, OP, and PG populations was described by Oliver et al. (2013), whereas stocks from the KO population were prepared as described by Wight et al. (2003), with further RNA removal as described by Tinker et al. (2014). DNA preparation for BG and PB was performed using a modified cetyl trimethylammonium bromide protocol as described by Babiker et al. (2015). For the AM population, DNA was prepared using DNeasy Plant (Qiagen, Venlo, Netherlands) extraction kits (Lin et al., 2014). For the 'IL86–1156' × 'Clintland 64' (IL4) and 'IL86–6404' × Clintland 64 (IL5) populations, DNA was prepared using a sodium dodecyl sulfate -based method modified from Pallotta et al. (2003).

Genotyping and Data Curation

Genotype data used in the present study included marker types from several platforms. All 12 biparental populations and monosomic hybrid lines were genotyped using the Oat 6K custom Infinium iSelect BeadChip (Illumina, San Diego, CA) assay reported by Tinker et al. (2014). For six populations (CH, HZ, KO, OP, OT, and PG) and the MHPs, we included SNP assays from two Illumina 1536-SNP oligo pooled assays from work previously reported by Oliver et al. (2013) when these were not redundant with the newer 6K array. All array-based SNP assays were performed using standard Illumina protocols at the USDA-ARS genotyping laboratory in Fargo, ND. Genotype calling of the oligo pooled assays and Infinium SNPs was initially performed using the genotyping module of GenomeStudio software version 2011.1 (Illumina), with GenCall set at 0.15. Since cluster separation parameters in GenomeStudio were not always effective in diagnosing tight but narrowly separated clusters affected by the dosage of homeologous markers, allele cluster positions were manually inspected, adjusted, and annotated for each SNP marker.

In addition to the oat SNP assay, AM was also genotyped using the wheat 90K iSelect BeadChip assay (Wang et al., 2014). Allele calling was performed as described by Lin et al. (2014). For 7 of the 12 populations, additional SNPs were assayed using GBS, in the manner previously reported by Tinker et al. (2014). For markers from all platforms, including historical markers from KO and OT (Portyanko et al., 2001; Wight et al., 2003), we applied stringent filtering criteria to obtain high-quality datasets (minor allele frequency ≥ 0.3, heterozygosity ≤ 0.1, call rate ≥ 0.9). The only exception was for the Infinium iSelect SNPs assayed in KO (minor allele frequency $\geq$

Table 1. Summary of oat genetic material.

Genetic material	Code	Pop.Size	Reference†	Number of markers (Illumina/GBS/Others)‡#	No. maps§	No. LG¶	No. mapped markers¶	Total length (cM) ¶
Kanota × Ogle (F_7)	KO	52	O'Donoughue et al. (1995)	3727 (1652/1237/838)	1	43	1914	2774.4
CDC Sol-Fi × HiFi (F_7)	CH	53	Oliver et al. (2013)	2387 (1437/950/na)	6	30 (23–38)	888 (494–906)	1196.1 (1174.2–1659.5)
Hurdal × Z-597 (F_6)	HZ	53	He et al. (2013)	2933 (1432/1501/na)	5	23 (27–35)	1508 (1222–1300)	1284.8 (1034.6–1383.6)
Ogle × TAMO-301 ($F_{6:7}$)	OT	53	Kremer et al. (2001)	6603 (2014/4063/526)	6	28 (20–37)	2257 (991–4140)	2393.2 (1410.9–2855.2)
CDC Boyer × 94197A1–9-2–2-5 (F_8)	BG	76	Babiker et al. (2015)	1111 (1111/na/na)	6	23 (20–28)	660 (497–698)	1479.6 (1043.9–2367.1)
Otana × PI269616 (F_6)	OP	98	Oliver et al. (2013)	4376 (1882/2494/na)	7	22 (22–33)	1166 (1036–2690)	1873.4 (1722.1–2086.7)
Provena × 94197A1–9-2–2-5 (F_8)	PG	98	Oliver et al. (2013)	3722 (1480/2242/na)	9	33 (36–43)	1821 (1230–1881)	2533.6 (1733.6–3479)
IL86–1156 × Clintland 64 ($F_{5:8}$)	IL4	112	Foresman (2014)	924 (924/na/na)	22	23 (19–26)	623 (350–572)	1057.6 (584.1–1170.5)
Provena × CDC Boyer (F_8)	PB	139	Babiker et al. (2015)	874 (874/na/na)	6	27 (26–32)	598 (385–564)	1613.1 (1219.1–1868.3)
Dal × Exeter ($F_{5:8}$)	DE	145	Hizbai et al. (2012)	2346 (935/1411/na)	6	25 (13–31)	895 (413–1326)	1165.7 (586.1–1858.1)
AC Assiniboia × MN841801 (F_7)	AM	161	Lin et al. (2014)	1688 (1196/na/492)	6	33 (30–38)	1366 (1153–1381)	1652.7 (1336.9–1738.7)
IL86–6404 × Clintland 64 ($F_{5:8}$)	IL5	171	Foresman (2014)	964 (964/na/na)	21	25 (25–38)	608 (375–579)	823.7 (372.9–1338.8)
Monosomic hybrid lines	MHP	51	Oliver et al. (2013)	1932 (1932/na/na)	na	na	na	na

† First publication using the population.

‡ Number of markers. For mapping populations, markers met the criteria of minor allele frequency ≥ 0.3, heterozygosity ≤ 0.1, call rate ≥ 0.9. For MHP, the number of polymorphic markers with a single-locus cluster profile is shown.

§ Number of maps generated and averaged for this population.

¶ Final number of linkage groups (LGs), number of mapped markers, and length of component maps produced for each population. The ranges of numbers from independent mapping replicates before merging are shown in parentheses. In some cases, the final numbers fell outside these ranges because of the merging procedure.

GBS, genotyping-by-sequencing; na; not applicable.

0.3, heterozygosity ≤ 0.1, call rate ≥ 0.7), because only 41 lines from this population were genotyped using this platform. The SNP marker phase was systematically checked and determined as described by Tinker et al. (2014).

Component Map Construction

Linkage maps were built using the MultiPoint package (MultiQTL Ltd., Haifa, Israel). A community-based mapping procedure was used, such that maps were averaged across a team and outlying outcomes could be detected and addressed. Variation among map outcomes are primarily a result of the different subsets of markers included, which were selected on the basis of interactive decision points described in the steps below. For each population, at least five maps were built by different people following these steps: preliminary grouping and ordering were conducted at recombination fraction (*rf*) = 0.15. Markers with *rf* = 0 were first binned together ("bound markers together" option) and markers with the fewest missing data were assigned as "delegates" to represent the bin. The reliability of marker order was checked through jackknife resampling: the probability of marker order was estimated based on 10 to 30 calculations, each one resulting from 90% of the population being sampled without replacement. Markers causing unstable neighborhood order were removed iteratively one at a time, on the basis of the variance of marker occurrence in a given position, the segregation ratio, and the *rf* with nearby markers. The ordering and marker removal sequence was repeated until the given linkage group showed a stable marker order. Linkage groups were merged end-to-end by incrementally increasing *rf* by 0.05 up to a final *rf* of 0.3. Maps constructed by different people based on the same data generally showed slight variation as a result of personal judgment during iterative marker ordering. Large variations could easily be attributed to errors and corrected. Following initial mapping, teams of five evaluated their linkage groups from individually constructed maps and chose the linkage

groups that represented the consensus of the team. Although there was some variation among maps, much as you would expect in an automated heuristic approach, the best map order was readily identifiable as the consensus. These selections were based on quality (length of linkage groups) and the frequency with which that solution was derived (a winner-takes-all approach). The same approach was used for each population with the exception of KO, which was produced once using MultiPoint with the same parameters but by a single individual.

Consensus Map Construction

Homologous linkage groups across 12 genetic maps were identified using an iterative approach combining distance-based clustering, merging within clusters, and manual inspection of the results (consensus versus component linkage maps). Based on previous work (Tinker, 2010), a distance metric (d) was developed to quantify the collinearity between every pair of linkage groups, taking into account the number of shared markers, the similarity of marker order, and the length of the shared region:

$$d = \frac{\sum_{i=1}^{n} \left(L_{iA} - L_{iB}\right)^2}{n},$$

where n is the number of markers shared by the two linkage groups (A and B) and L_{iA} and L_{iB} are the relative positions of the i^{th} shared marker on Map A or Map B, respectively. The relative positions were estimated by scaling the shared region of each linkage group (i.e., from the first shared marker to the last) to a length of unity, then using the scaled coordinates. Each pair of linkage groups was tested in two orientations (direct and flipped) and the highest value of d was used as the collinear distance.

An initial clustering using nearest-neighbor joining among all available component linkage groups across all populations was done using the following joining parameters: number of shared loci ≥ 5, length of the longest shared interval ≥ 15 cM, and $d < 0.1$. These thresholds were established through recursive optimization to give 21 initial clusters. Following this, all component linkage groups belonging to the same cluster (i.e., potential homologs) were merged using MergeMap (Wu et al., 2008) to create the consensus of that particular linkage group. For each consensus group, the merging of all contributing component linkage groups was performed simultaneously, with linkage groups weighted by population size. The marker orders between the resulting consensus and component linkage groups were then compared using dot-plots. Visual inspection of dot-plots allowed us to add or remove some component linkage groups from the distance-based clustering. For example, component groups that joined two otherwise separate clusters were removed, but short linkage groups that matched well despite not meeting the threshold were added. This cycle was repeated until the marker order of the consensus linkage groups showed consistency with all 12 mapping populations based on the dot-plots.

Following this, we used an in-house algorithm named Smooth Map Unitization by Slope Heuristics (SMUSH) to adjust each marker interval in the consensus to match the average component map distances for that region. This was done because the MergeMap algorithm is known to produce nonlinear inflated consensus distances when merging component maps with large numbers of nonshared markers (Close et al., 2009; Muñoz-Amatriaín et al., 2011). The SMUSH algorithm plotted all shared points on the consensus map versus the corresponding points on each matching component map. Orientations were adjusted (flipped as needed) and points were centered independently for each component map. Each interval on the consensus was scaled on the basis of the slope of the regression line fitting all points within a 40-cM window. The result of this adjustment was that new slopes calculated in 40-cM windows were very close to unity; in other words, the consensus distances were scaled to average component distances within that region. The SMUSH algorithm was written in Pascal and is available from the authors by request.

After consensus map scaling, we placed all remaining markers that had segregation data in at least one population back on the framework consensus using the following procedure: for each unplaced marker, we computed its average *rf* with all framework markers on the consensus based on all progeny with data for both markers. We then found the framework marker with the smallest average *rf*. Next, we selected the adjoining neighbor marker with the smallest average *rf* and placed the new marker at a position between these two markers at a cM position that was scaled proportionally to the two fractions, such that the framework interval was not altered. When the smallest *rf* was at a terminal framework marker, and that distance plus the distance to the subterminal framework marker was greater than the corresponding framework interval, the marker was placed distal to the terminal marker using the Haldane mapping function. In all cases, the framework coordinates (starting with zero) were preserved, such that it was possible to have negative coordinates for placed markers.

Chromosome Assignment

Assignment of physical chromosome nomenclature to consensus chromosomes was performed using F_1 chromosome-deficient hybrids derived from monosomic chromosome stocks, as described by Oliver et al. (2013). Briefly, monosomic stocks in either Sun-II or Kanota were used as a maternal parent, with Ogle or TAM O-301 as pollen parent, to produce a series of F_1 monosomic hybrid seeds that were grown and sampled as MHPs. The parents (Sun-II, Kanota, Ogle, and TAM O-301) and MHPs were assayed using the 6K SNP array and the subset of markers that were polymorphic between two parents (e.g., Sun-II and Ogle) and their associated MHPs were investigated. Since the critical monosomic chromosome usually forms a univalent laggard that is lost through the two meiotic divisions, the MHP is

expected to include only the alleles from the pollen parent in a hemizygous state (appearing as a homozygous phenotype) on the critical chromosome. All remaining markers from disomic chromosomes that were polymorphic between the parents are expected to appear as heterozygotes. If all or most of the qualifying markers from a consensus chromosome assayed in a given MHP were in a hemizygous state, while most markers from other linkage groups were in the heterozygous state, that consensus was assigned to the critical chromosome of the corresponding monosomic stock.

Most of the MHPs used by Oliver et al. (2013) were assayed in the current work using residual DNA samples. Where possible, genotypes from the previous SNP arrays were used to confirm or supplement the new scores from the 6K iSelect array. Only iSelect SNPs showing single-locus clustering were used for chromosome assignment. Where conflicts existed, data from the iSelect array were used in the assignments. Additionally, the karyotype of some F_1 hybrids was retested to confirm the loss of the critical chromosome and to determine if other rearrangements might have affected the results. This was done using the *C*-banding protocol followed by Oliver et al. (2013).

To supplement and confirm the monosomic assignments, the reference sequences from SNP assays, as well as those from GBS markers, were blasted [using nucleotide basic local alignment search tool (BLASTn)] against draft shotgun assemblies (to be published elsewhere) of an A-genome diploid accession (Cc7277 of *Avena atlantica* Baum & Fedak) and a C-genome diploid accession (CN21405 of *Avena ventricosa* Balansa ex Coss.). Markers meeting an e-value of 1×10^{-35} were assigned to the subgenome lineage to which they were most closely related. Based on these matches, chromosomes were assigned to the A or C genome when there was a clear majority of matches to one or the other. Since the A genome sequence was more complete than the C genome sequence, a greater density of A genome matches was expected, which was taken into account in the assignment of chromosomes. Assignment of partial chromosomes (i.e., an A–C genome split) was made when there was a clear alternation from the A genome to the C genome.

Oat-to-Oat Matching for Homeolog Inference

A self-against-self BLASTn (version 2.2.30, National Center for Biotechnology Information, Bethesda MD,) was conducted using the longest available sequence from each marker with an e-value less than or equal to 10^{-20} for each query sequence. Filtering was performed to exclude matches on the same chromosome and to exclude markers that matched markers on more than three other chromosomes. Chromosome positions of query and subject markers were rounded to the nearest cM and multiple matches for a given query marker that were within 1 cM on a subject chromosome were counted once. The total number of reciprocal matches (N) between two chromosomes was tallied, and $(N + 1)^{-1}$ was used as a distance metric between each pair of chromosomes. These distances were used in a minimum distance cluster analysis to identify groups of chromosomes with shared marker similarity. A second procedure, using a heuristic algorithm that provided smoothed inferences with regional continuity, was used to find the most likely and second most likely homeolog for localized chromosome regions. The algorithm used a sliding window of 30 cM on a query chromosome to tally the number of matches to each subject chromosome. The winning subject chromosome for each cM on the query chromosome was declared if it exceeded four matches. A second-place runner-up was declared if it was within 20% of the winner and also exceeded four matches. The result of this automated procedure was inspected and adjusted manually to estimate more accurately the beginning and ending points for each match, to remove gaps, and to add reciprocal matches when thresholds were met in only one direction between a pair of chromosomes.

Rice Ortholog Matching and Synteny Inference

Oat-to-rice matches were identified by performing tBLASTx and BLASTn (version 2.2.30, NCBI) searches of the longest available oat marker sequences against the masked pseudochromosome molecules from rice assembly version 7.1 (http://rice.plantbiology.msu.edu/annotation_pseudo_current.shtml, accessed 9 Mar. 2016), with an e-value of 10^{-20}. Filtering was performed to exclude markers that matched positions on more than two rice chromosomes. The chromosome positions of rice matches were rounded to the nearest 1×10^5 bp and multiple matches within this rounding unit were counted once. A heuristic algorithm was applied to provide a smoothed regional inference regarding the best and second-best rice matches. The algorithm used a sliding window of 30 cM on each oat chromosome to tally the number of matches to each rice chromosome. For each cM on the oat chromosome, the best rice chromosome match was declared if it exceeded four matches. A secondary region was declared if the number of matches was within 20% of the winner and also exceeded four matches. Rice matches and other annotations were visualized using Circos software (Krzywinski et al., 2009).

Data Availability

All mapping data have been provided in Supplemental Table S1. Maps are also available from the online database T3/Oat (http://triticeaetoolbox.org/oat/, accessed 9 Mar. 2016). Marker sequences are available in prior publications (Tinker et al., 2014) as well as in the T3/Oat database.

RESULTS AND DISCUSSION

Construction of Component Linkage Maps for Each Mapping Population

A de novo component map was constructed for each contributing population from all available data and without bias from pre-existing maps. For 11of 12 populations, a

community-based approach was used to construct a representative map based on 5 to 22 maps built by different individuals. We consider that the team-based approach added a valuable quality control to the end result of this work. Most mapping software, including MultiPoint (MultiQTL Ltd., Haifa, Israel), provides decision points, allowing for variation in final maps. The variation in the outcomes from those decisions is shown in Table 1. Such variation is typical for a large genome with a high density of molecular markers: it primarily reflects different densities and subsets of included markers and the cumulative pairwise distances thereof. Our approach allowed us to observe and address outlying maps (sometimes resulting from errors) and to provide component maps that were the average of multiple solutions. Despite the range of initial maps, the number of linkage groups and the total length of the final representative maps were similar to those of previous maps in hexaploid oat (Portyanko et al., 2001; Wight et al., 2003; Oliver et al., 2013). An exception was the map for IL5, which had a substantially shorter length (823.7 cM), possibly because of reduced genetic diversity. For some maps (HZ, IL4, PB, and IL5), the final versions contained more markers than the original maps because of the process of combining maps.

Marker intervals on the component maps ranged from 0.2 to 39.5 cM across the 12 maps. Depending on the population, 56.6 to 85.9% of the intervals were ≤5 cM, and large gaps (>30 cM) were present only in the BG and PB maps. The size of the largest gaps can reflect marker density and marker distribution, as well as population size. The BG and PB maps had some of the lowest marker densities (Table 1) but with population sizes that were adequate to detect such gaps. In most cases, each locus on the map was represented by a single marker; however, some markers were clustered at single map positions. The largest example is a cluster of 175 markers on the OT map. This is likely to be a result of high marker density as well as a small population size, which results in lower mapping resolution.

Assembly and Evaluation of the Consensus Map

Two sets of iterations of distance-based clustering, merging, and visual inspection of dot-plots were used to develop a final set of 21 primary consensus chromosome representations. Linkage groups that are the consensus of the underlying component maps are designated by Merge (Mrg), with the final set of primary representations referred to as Mrg 01 to Mrg 33. Each primary consensus group was developed from component linkage groups belonging to 4 to 12 different populations, with an average of nine component linkage groups from eight populations per group (Table 2). The numbering of these groups is arbitrary, reflecting only the order in which the clusters were formed. Alternate merged assemblies (Mrg 11v and Mrg 24v) were made for two clusters that contained three or four component populations but appeared to contain significant deviations from a primary consensus group (Mrg 11 and Mrg 24, respectively) containing a greater number of components. No other alternate clusters with three or more component groups were produced, although smaller clusters (containing two or three short linkage groups) or singletons could potentially be formed. These variations from the consensus could be either statistical artifacts or true physical differences in the chromosome structure found in a subset of the parental lines (see later discussion). After adjusting the length of the merged chromosomes to match the average length of the component groups and excluding the alternate versions, the total length of the merged map was 2843 cM and the average chromosome length was 135 cM (Fig. 1). The final merged consensus map is available in Supplemental Table S1 as well as in the online public T3/Oat database, where future updates may be made.

An example of the assembly of component maps into Mrg 01 is shown in Fig. 2, with the remaining assembly diagrams shown in Supplemental Fig. S1. In assembling this consensus map, we tried to err on the side of quality and certainty at the expense of including the maximum possible number of component groups in each merged consensus group. Thus, although Fig. 2 and Table 2 show that all 12 component populations contributed to Mrg 01, this was only true for two other chromosome representations (Mrg 08 and Mrg 21 in Supplemental Fig. S1). After this conservative merging process, it was found that the majority of component linkage groups showed a high degree of collinearity with a single merged consensus, as illustrated in Fig. 3 and continued in Supplemental Fig. S2. An alternative dot-plot comparison (Supplemental Fig. S3) between consensus groups and all possible component groups illustrates the same point. In most cases, the inclusion of additional components in the merging process would have produced a similar map but with increased ambiguity in marker order, which is an undesirable outcome, as our goal was to be most representative of these 12 populations.

Although there were some significant deviations between the consensus and some linkage groups from individual maps (discussed later), we are confident that the map presented here is a robust representation of chromosome membership and marker order in most cultivated *A. sativa* germplasm. Furthermore, we assembled this consensus map using methods that were as objective and reproducible as possible, and without bias or influence from previous oat maps. Importantly, the current consensus was built through a merging algorithm that acted simultaneously on all component linkage groups and which could be systematically repeated, rather than being based on many stepwise iterative alignments in which the starting point could influence the outcome. Thus, it was reassuring that, despite the much larger number of markers and six additional component maps, most consensus chromosomes matched approximately with those in the previous consensus map (Oliver et al., 2013). This similarity is illustrated graphically by a dot-plot comparing the current and previous maps

Table 2. Properties of consensus chromosomes and contributing merged component linkage groups.

Group	Length†	Total Markers‡	Number of component groups contributing to each consensus group												
			No.§	AM	DE	BG	HZ	IL4	IL5	KO	OP	OT	PB	PG	SH
Mrg 01††	143	667	14 (12)	1	1	1	1	2	1	1	2	1	1	1	1
Mrg 02	132	205	4	1	–	–	–	–	1	1	1	–	–	–	–
Mrg 03	168	472	13 (10)	2	1	1	1	–	2	1	1	–	1	2	1
Mrg 04	80	287	8	1	1	–	1	–	–	–	1	1	1	1	1
Mrg 05	175	428	9	1	–	1	1	1	1	1	1	1	–	1	–
Mrg 06	147	206	6	–	–	1	–	–	–	1	1	1	1	1	–
Mrg 08	195	506	14 (12)	1	1	2	1	1	2	1	1	1	1	1	1
Mrg 09	136	324	11 (10)	1	1	1	1	1	1	–	1	2	1	–	1
Mrg 11	126	337	5	1	–	–	1	–	–	–	1	1	1	–	–
Mrg 11v¶			4	1	–	–	1	–	–	–	–	1	–	–	1
Mrg 12	119	372	11 (10)	2	–	1	1	1	1	1	1	–	1	1	1
Mrg 13	119	438	7	1	–	–	1	–	–	1	1	1	1	1	–
Mrg 15	91	234	5	1	–	–	–	–	1	1	1	–	1	–	–
Mrg 17	122	482	15 (11)	1	1	1	1	1	2	–	1	1	2	2	2
Mrg 18	90	209	8	1	1	1	–	1	1	–	–	1	1	1	–
Mrg 19	92	218	15 (11)	2	1	2	–	1	1	1	1	1	2	1	2
Mrg 20	261	472	14 (10)	2	1	2	1	–	1	1	1	–	1	2	2
Mrg 21	212	457	13 (12)	1	1	1	1	1	1	1	1	1	1	1	2
Mrg 23	111	289	10	1	1	1	1	–	–	1	1	1	1	1	1
Mrg 24	95	267	9 (8)	–	1	–	1	1	1	–	1	1	1	–	2
Mrg 24v¶			3	1	–	1	–	–	1	–	–	–	–	–	–
Mrg 28	96	252	6	–	1	–	–	–	1	–	1	1	1	1	–
Mrg 33	133	146	4	1	–	–	–	–	–	–	1	1	1	–	–
Total	2843	7268	208 (185)	20	13	14	15	10	16	13	20	17	19	15	13
Average#	135	347	9 (8)	1.2	1.0	1.2	1.0	1.1	1.2	1.0	1.1	1.1	1.1	1.2	1.4

† Length after heuristic scaling to match component maps.

‡ Total markers in the merged consensus before ad hoc placement of additional markers.

§ Number of contributing component groups (the number of contributing populations is shown in parentheses if different).

¶ Alternate versions of Groups 11 and 24 containing component groups in which the marker order differed substantially from the major version.

Total and average length, number of markers, or number of contributing component groups.

†† Mrg, Merge, used to indicate linkage groups that are the consensus of the underlying component maps; other two-letter codes for each population are explained in Table 1.

(Supplemental Fig. S4), as well as by a field in the text-based map annotating the positions of markers in the previous map (Supplemental Table S1). Despite these similarities, specific differences exist, such as the substantial revision of Mrg 11 (formerly chromosome 1C). An earlier effort at merging the current 12 component maps through a stepwise procedure similar to that used by Oliver et al. (2013) produced similar differences, which we attributed to starting with maps that were atypical for specific chromosomes (data not shown). The framework of the present consensus map contains sevenfold more markers than the previous map. It also covers an additional 1000 cM, after correction to remove the inflation caused by MergeMap. Despite this, the predicted and highly stable number of chiasma in typical oat varieties is approximately 42 (Baptista-Giacomelli et al., 2000), suggesting an expected average chromosome length of 200 cM. Thus, the current map may still reflect an undersampling of the full oat genome, possibly caused by an undersampling of markers in telomeric regions. Where differences from prior maps exist, we consider the current map to be representative of more component maps and their underlying populations. This new consensus framework is an important improvement over previous work and is a key foundation for new work based on high-throughput SNP markers.

Chromosome Assignment

After merging component linkage groups into a consensus, it was assumed that each merged group represented a full chromosome in the most typical physical configuration found in spring oat germplasm. The MHPs were then used to nominate the most likely physical chromosome assignment for each consensus chromosome. New 6K iSelect SNPs, as well as those from previous assays (Oliver et al., 2013), were filtered to identify polymorphisms in monosomic hybrids and their parents, with clear cluster separation allowing unambiguous differentiation between heterozygous and hemizygous states. A difficulty arose after it was determined that the

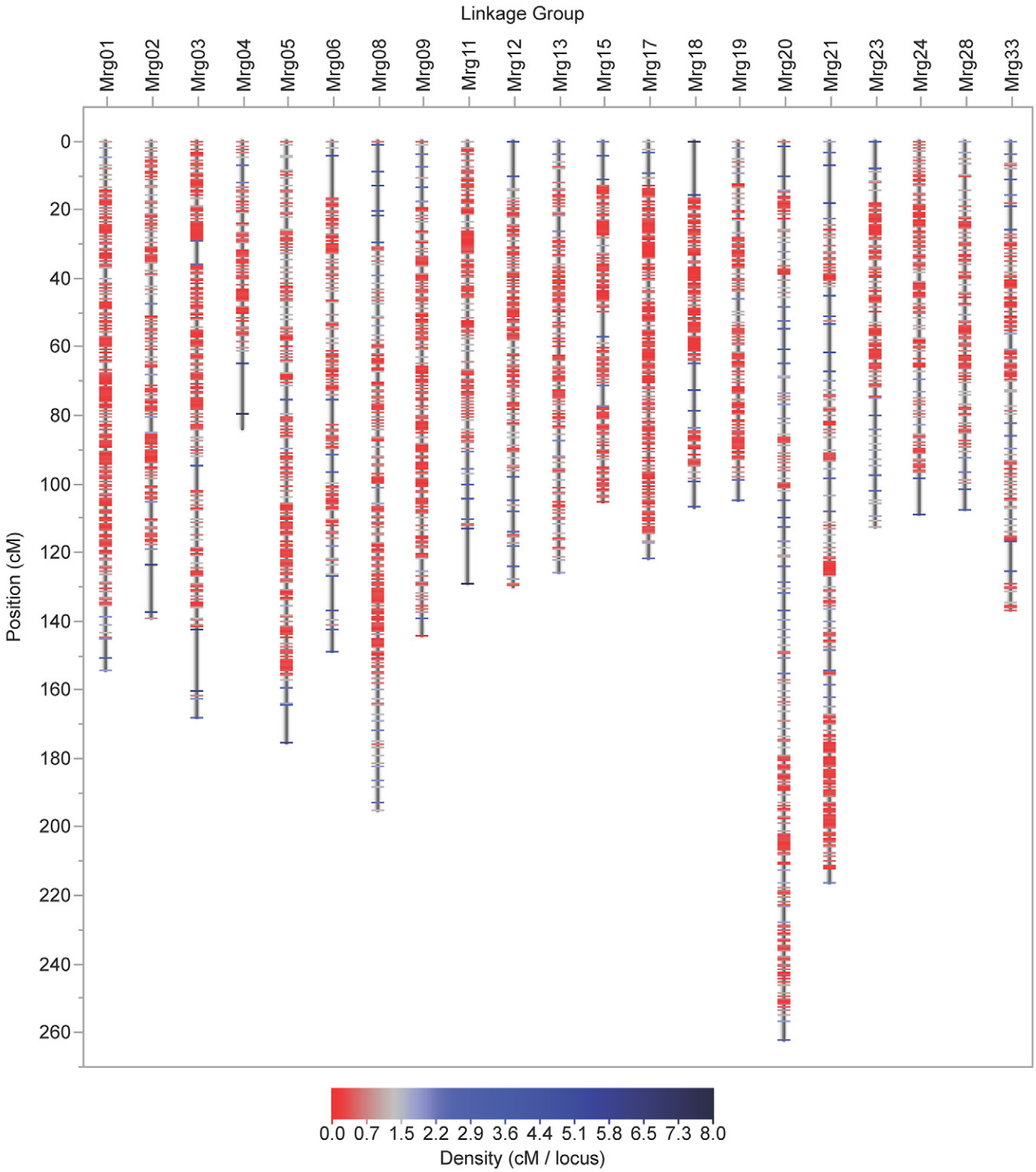

Fig. 1. Overall representation of the hexaploid oat consensus map based on 12 mapping populations and 19 oat varieties. The vertical scale is in cM. The horizontal scale indicates the resulting group assignment. Linkage groups that are the consensus of the underlying component maps are designated by Merge (Mrg). Tick marks represent the position of one or more markers; marker density is represented by a color gradient where red is the highest marker density and blue is the lowest density (see gradient density legend).

samples identified as Kanota and TAM O-301 were likely mislabeled. Thus, parental genotypes were inferred, where possible, for the resulting MHPs, and were cross-validated in paired MHPs from the Ogle parent. Furthermore, many markers were not diagnostic because their heterozygous state was confounded by simultaneous interrogation of a homeologous locus, as discussed by Tinker et al. (2014). Thus, the final chromosome assignments were based conservatively on 221 diagnostic hemizygous loci that were scored on the 6K array and

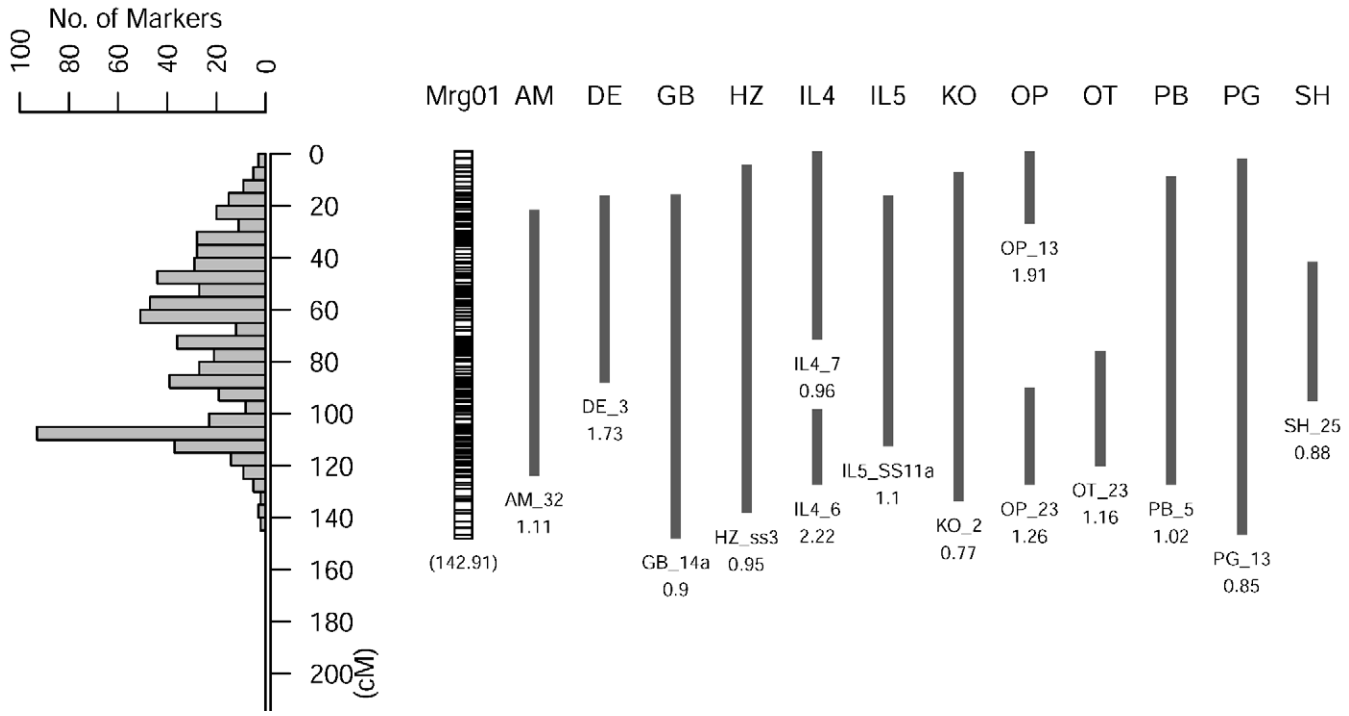

Fig. 2. Merging of component linkage groups into the Merge (Mrg) 01) oat chromosome representation. The vertical units are in cM. Vertical bars show regions where a component linkage group that was used in the assembly matched the final merged consensus. Numbers underneath the component linkage groups indicate the factor by which each contributing linkage group would need to be stretched or compressed to match the corresponding first and last markers on the final merged consensus. Similar diagrams for the remaining 20 merged groups are shown in Supplemental Fig S1.

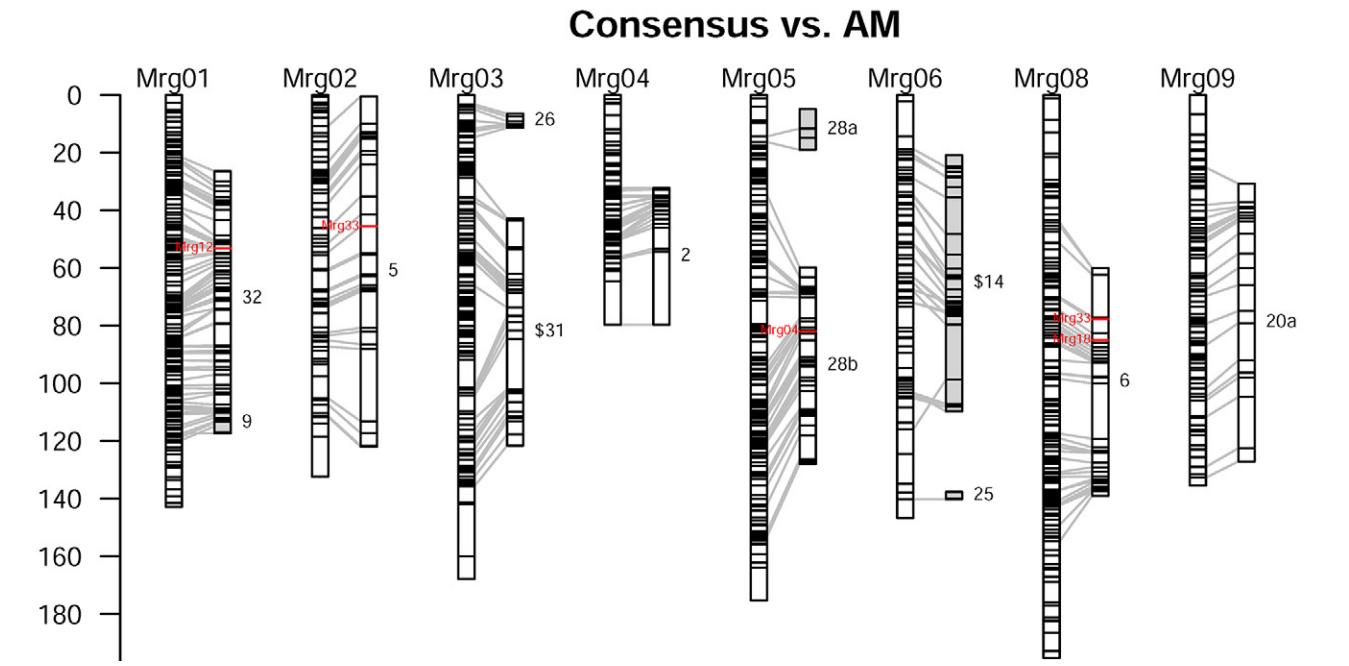

Fig. 3. Collinear matching for 11 of the component chromosome representations (labels on right) from the *A. sativa* AC Assiniboia × MN841801 (AM) population to eight groups (Mrg 01 to Mrg 09) in the final consensus map. Vertical scale is in cM. Red labels indicate markers that mapped to alternate merged assemblies. Dollar symbols ($) indicate that the component group is flipped relative to the original component map. Shaded component groups (9, 28a, $14, and 25) did not meet thresholds for inclusion in the primary merge but are shown next to the merged consensus with the greatest similarity. Collinear matches for the remaining component groups in AM, as well as those from 11 additional contributing maps, are provided in Supplemental Fig. S2.

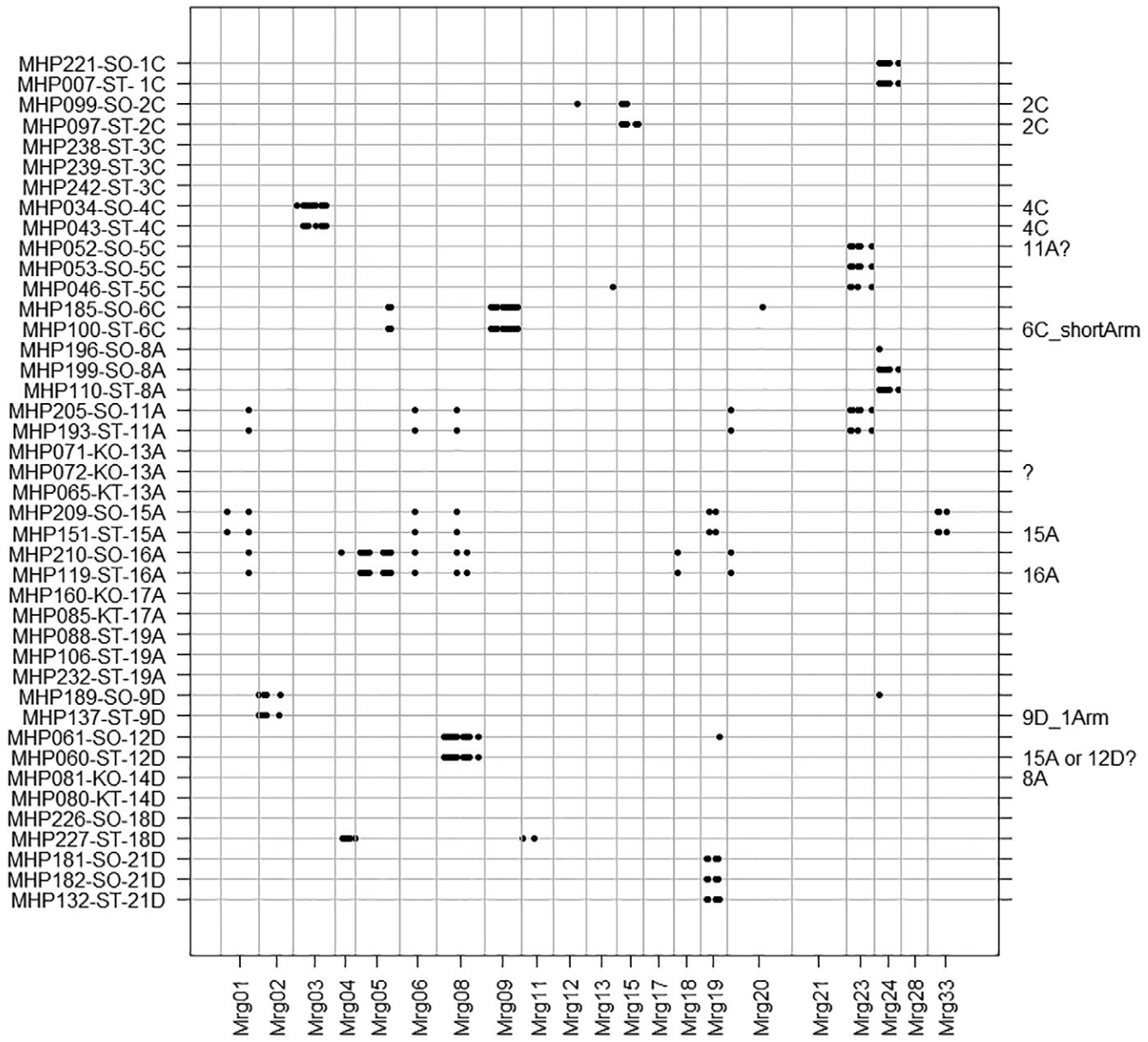

Fig. 4. Matrix of monosomic hybrid plant (MHP) identities based on diagnostic markers used for physical chromosome assignments in oat. Monosomic hybrid plant lines are identified on the left axis along with their targeted critical chromosome, based on the karyotype of the original monosomic stock used as a female parent in production of the hybrid. Karyotype confirmations performed in the MHP plants are shown on the right when available. A total of 221 black dots indicate the diagnostic homozygous phenotypes (inferred hemizygotes) of markers that are heterozygous in the remaining MHPs from the same parental series. Regions containing high densities of overlapping markers were used in the chromosome assignments shown in Table 3.

were consistent with previous assays. The resulting grid of diagnostic markers used for chromosome assignment is illustrated in Fig. 4. Physical chromosome assignments were made when a consensus chromosome contained a clear stretch of markers that were hemizygous in one or more MHPs that represented a single monosomic chromosome. For example, most of Mrg 03 was covered by diagnostic hemizygous markers in MHP 34 and MHP 43, both of which targeted chromosome 4C. The karyotype of MHP 34 was reconfirmed (Fig. 5A) and was found to be monosomic for chromosome 4C. Thus, we have assigned Mrg 03 to physical chromosome 4C.

Three of the 12 monosomic reconfirmations listed in the right-hand margin of Fig. 4 did not give results that were consistent with the targeted critical chromosome. These included MHP 81 (Fig. 5B), MHP 052, and MHP 072. The results from these chromosomes were not applied to the assignments shown in Table 3.

Nine chromosomes were assigned with this reasonably high level of certainty (Table 3) and all of these were consistent with the corresponding chromosome assignments inferred by Oliver et al. (2013). All of these assignments were also consistent with the subgenome identity of either A–D or C, as assigned on the basis of

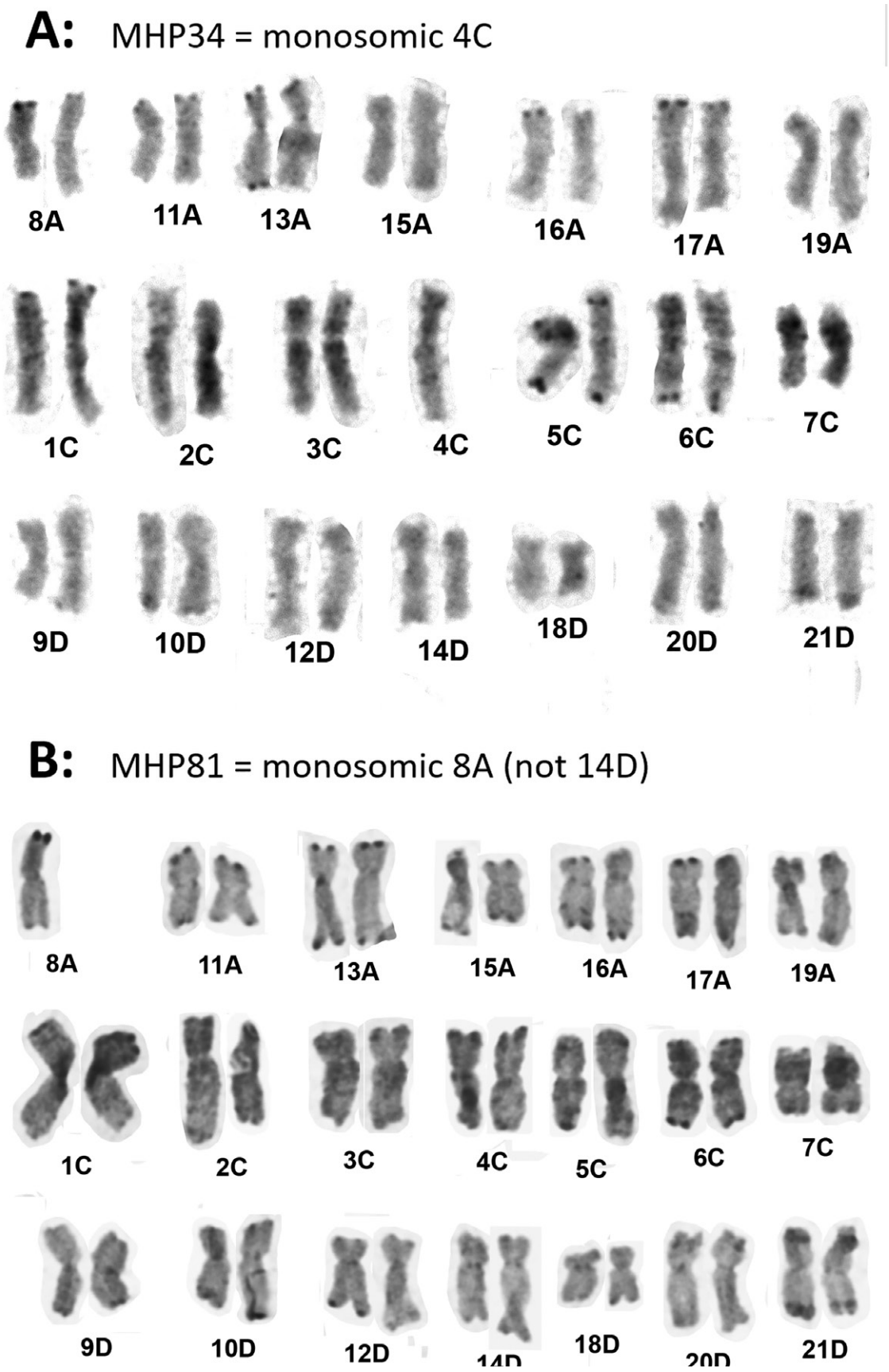

Fig. 5. Karyotyped *C*-banded cells from monosomic hybrid progeny MHP 34 (A) and MHP 81 (B), confirming the presence of monosomic chromosomes 4C and 8A, respectively. In the case of MHP 34, 4C is the targeted critical chromosome, based on the monosomic stock from *Avena sativa* Sun-II; in MHP 81, the targeted chromosome was 14D from a monosomic stock in Kanota. Magnification is 1000×.

Table 3. Current assignment of merged chromosomes to physical chromosomes, previously assigned nomenclature, and supporting evidence for revised assignments.

Merged group	Assigned†	MHP†	Oliver 2013‡	KO DArT§	Diploid¶
Mrg 01			5C (conflict)	KO_5_30	A
Mrg 02	9D	137, 189	9D	KO_17	A
Mrg 03	4C	34, 43	4C, 10D	KO_32	C
Mrg 04	18D	226, 227	18D	KO_33	A
Mrg 05	16A	119, 210	16A, 1C	KO_24_26_34 + 11_41_20_45	A
Mrg 06			14D	KO_5_30 + KO_14	A/C
Mrg 08	12D	60, 61	12D	KO_2 + KO_47	A/C
Mrg 09	6C	100, 185	6C	KO_29_43 + KO_7_10_28	C
Mrg 11			1C	KO_21_46_31_40 + 11_41_20_45	C/A
Mrg 12			13A	KO_6	A
Mrg 13			20D (conflict)	KO_8	C
Mrg 15	2C	97, 99	2C, 10D	KO_15	C
Mrg 17			3C	KO_36, KO_42	C
Mrg 18			7C-17A	KO_1_3_38_X2	C
Mrg 19	21D	131, 181, 182	21D	KO_4_12_13	C/A
Mrg 20			19A	KO_22_44_18	A
Mrg 21			16A	KO_24_26_34 + 11_41_20_45	A/C
Mrg 23	11A	52, 193, 205	11A	KO_4_12_13	A
Mrg 24			8A, 14D	KO_16_23	A
Mrg 28			7C-17A	KO_1_3_38_X2	C
Mrg 33		151, 209	15A	KO_7_10_28 + KO_17	A

† Confirmed assignments are based on consistency of hemizygous state in designated monosomic hybrid lines [monosomic hybrid plant (MHP) identifiers]. The karyotype of MHP lines that are underscored were reconfirmed directly in the diagnostic hybrid. Other MHP lines were inferred by using the pedigree of the original monosomic parent stock.

‡ Corresponding chromosome in the map of Oliver et al. (2013) based on shared loci. Chromosome names in the 2013 map were based on physical chromosome assignments that may not be correct. Those labeled "conflict" show conflicting evidence to the assignment based on matches to diploid genomes. Those underlined are supported by new assignments. The remaining designations are not in dispute but there is no longer adequate evidence to make the assignment.

§ Corresponding linkage groups in the Diversity Array Technology (DArT)-based map in Kanota × Ogle (KO (Tinker et al. (2009), based on shared markers.

¶ Predominant diploid genome assignment of markers in the new merged consensus group based on sequence identity to draft shotgun genome sequences. Where assignments are split, the assignment given to the longest part of the chromosome is shown first. Assignments to the A genome may also reflect D genome chromosomes. A/C indicates that those merged linkage groups have matches to both the A and C diploid genomes and it is unclear which one is the strongest match.

the read matches in the diploid shotgun sequences (Table 3). However, assignments for the remaining 12 consensus chromosomes remain unknown or ambiguous according to the current data. In some cases, it appeared that a series of MHPs (e.g., MHP 65 through MHP 85) had lost fragments from multiple chromosomes. This was sometimes supported by karyotypes that showed the loss of multiple chromosomes and/or the possible rearrangement of chromosomes.

Although most of the MHP lines used by Oliver et al. (2013) were the same lines used in the current study, they assayed fewer markers using the pilot SNP arrays. Because of the smaller numbers of diagnostic hemizygous loci and because it was not then apparent that MHPs may have lost additional whole or partial chromosomes, some previous chromosome assignments were made that now appear ambiguous. In addition, since a complete series of MHPs was not available at the time, Oliver et al. (2013) based the designations of 1C, 5C, 7C–17A, and 17A–7C on previous work by Fox et al., (2001), who had built their assignments on a relatively small (average 3.7) number of markers per chromosome. Of these, we now have conflicting or ambiguous MHP assignment data for 1C and 5C, whereas the assignments of the translocated 7C–17A pair remain uncertain. The assignments of 3C and 10D were performed using DArT dilution analysis, which was not expanded in the current study. Three new MHPs from monosomic 3C do not support that previous assignment, whereas the previous incarnation of chromosome 10D was extremely small, with markers that are now represented in larger consensus groups. Some assignments that were made previously, using a smaller number of markers than was considered adequate in the current work, may still be correct. Since some of these previous assignments agree with the diploid sequence data (e.g., 13A, 3C) we have included the legacy assignments in Table 3 for cross-reference in future work. However, since there is now strongly conflicting evidence for at least two previous assignments (5C and 20D) based on diploid subgenome hybridization, and since some consensus chromosomes may actually be the true translocated versions of physical chromosomes, we advise caution in the future with respect to the use of chromosome designations. It is for this reason that we have elected to follow the arbitrary "Mrg" nomenclature assigned during consensus map construction. In some

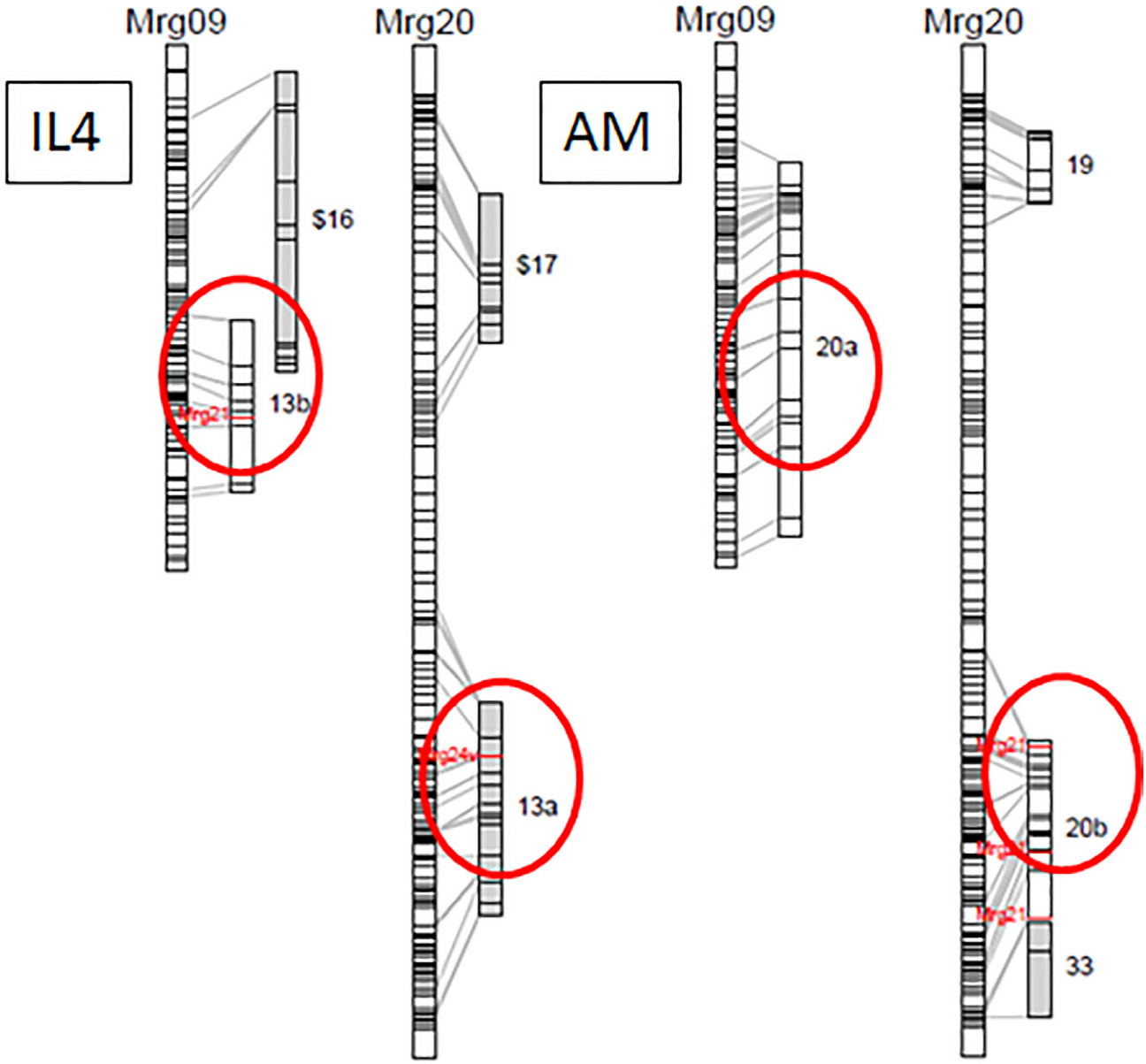

Fig. 6. Detailed alignment of component linkage groups from oat populations IL86–1156 × Clintland 64 (IL4) (13a and 13b) and AC Assiniboia × MN841801 (20a and 20b), which were split before merging because of recombination gaps. Consensus linkage groups (left) and component linkage groups (right) were linked where common markers are found. Component linkage groups in white are used for consensus merging; component linkage groups in gray did not meet the requirements for merging.

instances, when the comparison to previous work is relevant, we refer to assigned or previously assigned chromosomes in parentheses.

Genome Rearrangements Revealed During Consensus Map Construction

Genomic translocations have been documented between chromosomes 7C and 17A through previous cytogenetic work by Jellen et al. (1994). Although the presence of this translocation was known going into the merging process, it became apparent that there was probably more than one reciprocal rearrangement reflected in the heterogeneous chromosome configurations observed among component maps. For example, Fig. 6 shows that linkage group 13 from the IL4 population merges into both Mrg 09 (6C) and Mrg 20. Linkage group 13 from IL4 was split before merging (because a large >20 cM distance between internal markers), which resulted in the formation of 13a and 13b. The same thing is seen in the AM population (i.e., linkage group 20 merges into both Mrg 09 (6C) and Mrg 20). This linkage group was also split because of a large interval between internal markers. Although we cannot discount that this may be caused by false positive linkages in the component maps, the observation of this same rearrangement in two populations suggests that this is indeed a population-specific rearrangement. In another case, Linkage Group 2 from the DE population has a small piece on the end of the linkage group that contains markers that map to both Mrg 20 and Mrg 05 (16A). In this particular case, it is more likely that we

have duplicate markers on the distal end of this linkage group. To merge the rest of Linkage Group 2, which clearly belonged in Mrg 20, we removed the end of Linkage Group 2 and discarded those deleted sequences as ambiguous marker placements.

The merging of 12 populations into a consensus map presented several challenges, one of which was how to contend with rearrangements in specific populations. An initial approach to merging was an iterative merging process starting with populations that had recurrent parents, such as IL4 and IL5. Although this approach seems logical, it inadvertently introduces a bias in the merging process toward the component maps chosen for the first merge, which may not be representative of the majority of the germplasm. One option available in MergeMap is weighting: the user can define which maps they would prefer be given more weight in the merging process. Because the population size of the component maps varied greatly, we chose to weigh maps with a greater population size more heavily, the logic being that maps with more individuals allow for better resolution of conflicts and more accurate placement of markers.

Evaluation of the Map Based on Linkage Disequilibrium

The analysis of an oat population diversity study, reported in a companion paper (Klos et al., 2016), provided an opportunity to evaluate the present consensus map in relation to a genome-wide matrix of linkage disequilibrium (LD) estimates. This work showed that LD decayed in an expected linear fashion in relation to map distance along most consensus chromosome representations from the current map. Since the evaluated population contained mixed germplasm from diverse global origins, this provides evidence that the current map is a good representation of the majority of oat germplasm. Nevertheless, some chromosomes showed breaks from this pattern that may represent genomic regions where rearrangements are more common or where the map is less representative of the sample germplasm. In particular, Mrg 02 and Mrg 28 showed a preponderance of high LD estimates at distances beyond 10 cM, which may reflect diversity in the physical conformations of these chromosomes. In addition, Mrg 28 showed a slower rate of LD decay in spring oat than in southern germplasm but in all other chromosome representations, LD decayed more slowly in southern germplasm. Although Mrg 28 is an unconfirmed candidate for the 7C–17A translocated chromosome, Mrg 02 (confirmed as chromosome 9D) is not known to be translocated but the deviations could potentially reflect heterogeneity in other physical variations such as a heterogeneous inversion or introgression. For example, Wight et al. (2004) identified that the crown rust resistance gene *Pc38*, which was introgressed from a wild oat relative, mapped to KO 17 (equivalent to Mrg 02) in one cross but mapped to a different homeologous region in a second cross.

Map Saturation by Additional Marker Placement

Although there was a total of 16,880 markers mapped in at least one population, the framework consensus map contained only 7202 markers. Markers that were excluded from the framework were either on linkage groups that did not contribute to the merged framework or they mapped inconsistently and were discarded by the merging procedure. The ad hoc marker placement procedure was able to assign 9677 markers to a "best" position based on the consensus framework marker showing the lowest average recombination. Because these markers may have conflicting evidence for alternate placement and because we have excluded these markers from certain analyses, these markers are flagged (0 = non framework) in the text-based map (Supplemental Table S1).

It has been observed in previous work (e.g., Oliver et al., 2013) that inconsistent marker placement can result from at least two factors: (i) interrogation of different loci with similar sequence (potential homeologs) by the same assay in different populations or (ii) translocations or other rearrangements causing different linkages or pseudolinkages among populations. Because of this, we considered that an analysis of alternate placements could help to elucidate homeologous chromosomes and/or translocated chromosome pairs. An overall summary of alternate placements is shown in Fig. 7, with details by map position presented in Supplemental Table S2. The interpretation of these alternate placement data is best performed in relation to homeologous sequence matching and thus this is discussed in the following section.

We should also note that these marker mapping ambiguities should not be surprising, given that crossing among the largely interfertile hexaploid *Avena* taxa (*A. sativa*, including ssp. *byzantina*, and *Avena sterilis* L.) is a common feature in the pedigrees of most of the mapping parents used in this study. For example, a seven-generation ancestry interrogation of the pedigree of Ogle (pedigrees accessed through http://pool.aowc.ca, accessed 9 Mar. 2016) includes ancestors known to carry normal 7C and 17A from *A. sativa* ssp. *byzantina* landraces (e.g., 'Red Algerian' and 'Landhafer', among many others) along with *A. sterilis* material. In many cases, oat varieties have been successful because they carry resistance genes introduced from exotic germplasm sources. The cultivar CDC Boyer is similarly complex and includes the landrace 'Markische Landsorte', which harbors the 3C–14D rearrangement. The recent ancestry of 'Hi-Fi' includes the synthetic hexaploid 'Amagalon' (*Avena magna* H.C.Murphy & Terrell × *Avena longiglumis* Durieu) as the source of rust resistance genes *Pc91* and *Pg-a* (Rooney et al., 1994; McCartney et al., 2011). The parent 94197A1-9-2-2-2-5 of cross BG contains recent ancestry from *A. sterilis*; other wild oat ancestry can be found in pedigrees of these parents. The very high expected amount of genetic buffering in an allohexaploid plant may accommodate such wild introgressions as well as duplications and deficiencies arising from reciprocal and nonreciprocal chromosomal rearrangements.

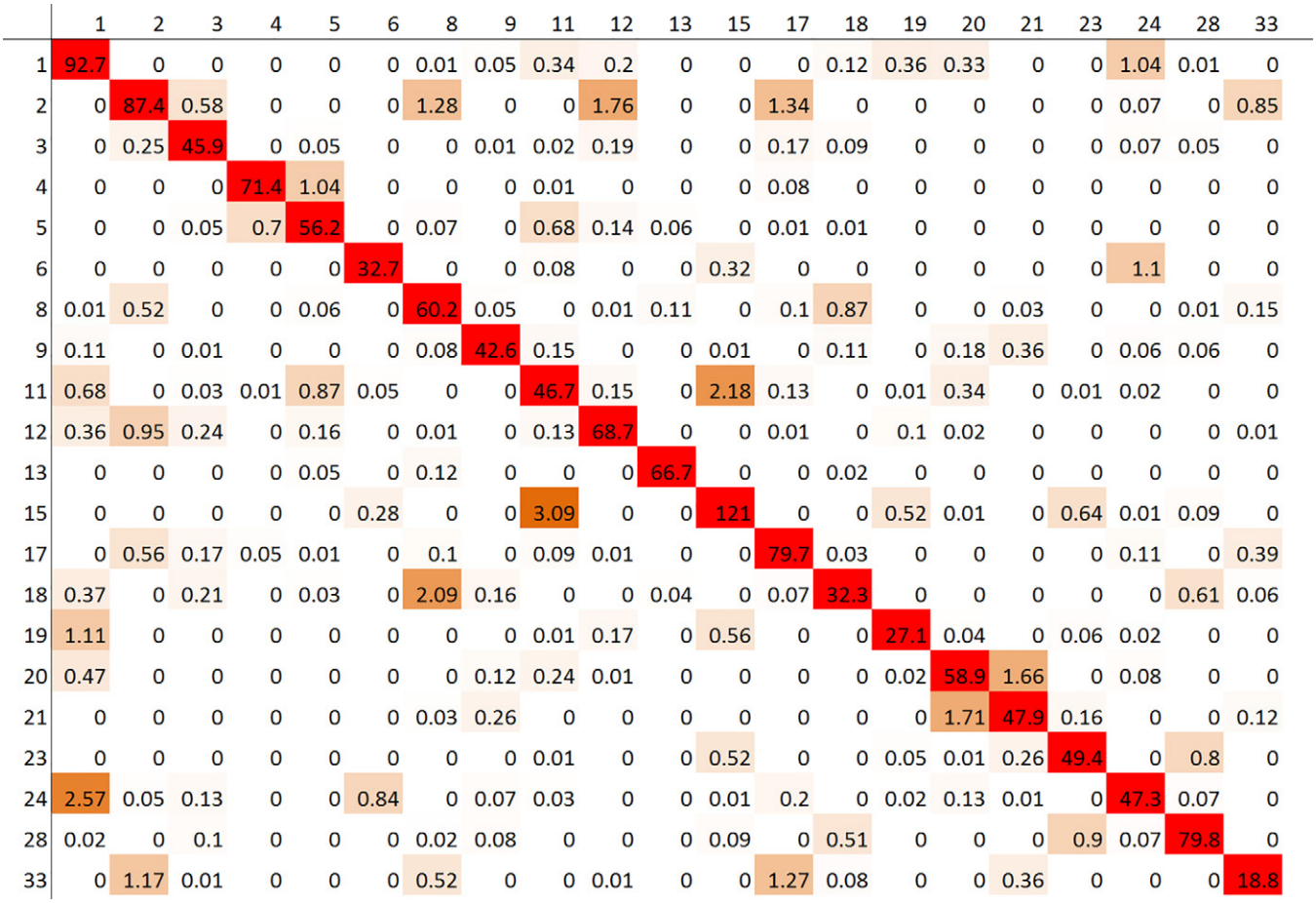

	1	2	3	4	5	6	8	9	11	12	13	15	17	18	19	20	21	23	24	28	33
1	92.7	0	0	0	0	0	0.01	0.05	0.34	0.2	0	0	0	0.12	0.36	0.33	0	0	1.04	0.01	0
2	0	87.4	0.58	0	0	0	1.28	0	0	1.76	0	0	1.34	0	0	0	0	0	0.07	0	0.85
3	0	0.25	45.9	0	0.05	0	0	0.01	0.02	0.19	0	0	0.17	0.09	0	0	0	0	0.07	0.05	0
4	0	0	0	71.4	1.04	0	0	0	0.01	0	0	0	0.08	0	0	0	0	0	0	0	0
5	0	0	0.05	0.7	56.2	0	0.07	0	0.68	0.14	0.06	0	0.01	0.01	0	0	0	0	0	0	0
6	0	0	0	0	0	32.7	0	0	0.08	0	0	0.32	0	0	0	0	0	0	1.1	0	0
8	0.01	0.52	0	0	0.06	0	60.2	0.05	0	0.01	0.11	0	0.1	0.87	0	0	0.03	0	0	0.01	0.15
9	0.11	0	0.01	0	0	0	0.08	42.6	0.15	0	0	0.01	0	0.11	0	0.18	0.36	0	0.06	0.06	0
11	0.68	0	0.03	0.01	0.87	0.05	0	0	46.7	0.15	0	2.18	0.13	0	0.01	0.34	0	0.01	0.02	0	0
12	0.36	0.95	0.24	0	0.16	0	0.01	0	0.13	68.7	0	0	0.01	0	0.1	0.02	0	0	0	0	0.01
13	0	0	0	0	0.05	0	0.12	0	0	0	66.7	0	0	0.02	0	0	0	0	0	0	0
15	0	0	0	0	0	0.28	0	0	3.09	0	0	121	0	0	0.52	0.01	0	0.64	0.01	0.09	0
17	0	0.56	0.17	0.05	0.01	0	0.1	0	0.09	0.01	0	0	79.7	0.03	0	0	0	0	0.11	0	0.39
18	0.37	0	0.21	0	0.03	0	2.09	0.16	0	0	0.04	0	0.07	32.3	0	0	0	0	0	0.61	0.06
19	1.11	0	0	0	0	0	0	0	0.01	0.17	0	0.56	0	0	27.1	0.04	0	0.06	0.02	0	0
20	0.47	0	0	0	0	0	0	0.12	0.24	0.01	0	0	0	0	0.02	58.9	1.66	0	0.08	0	0
21	0	0	0	0	0	0	0.03	0.26	0	0	0	0	0	0	0	1.71	47.9	0.16	0	0	0.12
23	0	0	0	0	0	0	0	0	0.01	0	0	0.52	0	0	0.05	0.01	0.26	49.4	0	0.8	0
24	2.57	0.05	0.13	0	0	0.84	0	0.07	0.03	0	0	0.01	0.2	0	0.02	0.13	0.01	0	47.3	0.07	0
28	0.02	0	0.1	0	0	0	0.02	0.08	0	0	0	0.09	0	0.51	0	0	0	0.9	0.07	79.8	0
33	0	1.17	0.01	0	0	0	0.52	0	0	0.01	0	0	1.27	0.08	0	0	0.36	0	0	0	18.8

Fig. 7. Heat map showing alternate marker placements by consensus oat chromosome pairs. Each column represents the chromosome of framework map location or primary placement, and each row represents alternate chromosome placements. Numbers in each cell represent the number of alternate placements (at ≤10% recombination) of markers from that column at an average position on the chromosome in that row. For example, the average framework marker on primary consensus chromosome representation (Mrg) 01 has 1.04 markers from Mrg 24 that could alternately be placed at that position, whereas the average framework marker on Mrg 24 has 2.57 markers from Mrg 01 that could alternately be placed at that position. The average marker on Mrg 01 also has 92.7 other markers from the same chromosome (which is likely to be adjacent) that could be placed there by the same criteria. These averages are calculated from the complete framework matrix shown in Supplementary Table S2, where regional trends in alternate placement can be seen. Color intensity is used to highlight higher numbers of alternate placements between chromosomes.

Oat-to-Oat Matching and Homeolog Inference

Direct matching among marker sequences was performed using BLASTn, resulting in a heat matrix showing pairs of chromosomes with high numbers of potentially homeologous markers (Fig. 8, Supplemental Table S3). Single distance cluster analysis, based on reciprocals as a distance metric, revealed groups of chromosomes with high degrees of similarity (Fig. 9). If three homeologous subgenomes of oat (A, C, and D) had been preserved intact, then we would expect to see a clear set of seven clusters, each with three chromosome members. Indeed, there appear to be two clusters containing three members that are separated by divergent joins (Mrg 20, Mrg 21, and Mrg 09, as well as Mrg 23, Mrg 15, and Mrg 28); however, most of the remaining chromosomes fall into two larger clusters that are not clearly delineated, plus two chromosomes (Mrg 08 and Mrg 13) that are not joined closely with any other groups. The cause of these nondiscrete clusters can be seen clearly in Fig. 10, where green ribbons show the conserved regions of matches among oat chromosomes that are ordered to correspond with the clusters in Fig. 9. Many of these inferred homeologous regions (Fig. 10) and groupings among chromosomes (Fig. 9) are in agreement with the homeologous relationships that were inferred by Gutierrez-Gonzalez and Garvin (2011) in the KO map using *Brachypodium distachyon* (L.) P.Beauv. as a reference. By comparing the results presented in figure 4 of Gutierrez-Gonzales and Garvin (2011) using the KO correspondence in our Table 3, we see that they also identified the strong homeology that we see among Mrg 23, Mrg 15, and Mrg 28 and among Mrg 20, Mrg 21, and Mrg 09, as well as between Mrg 12 and Mrg 02 and between Mrg 04 and Mrg 05. Although some of these relationships are now less fragmented than those observed by Gutierrez-Gonzalez and Garvin (2011) and despite large regions of synteny among Mrg 20, Mrg 21, and Mrg 9 that may indicate a conserved series of A, C, and D chromosomes, many of the remaining matches are

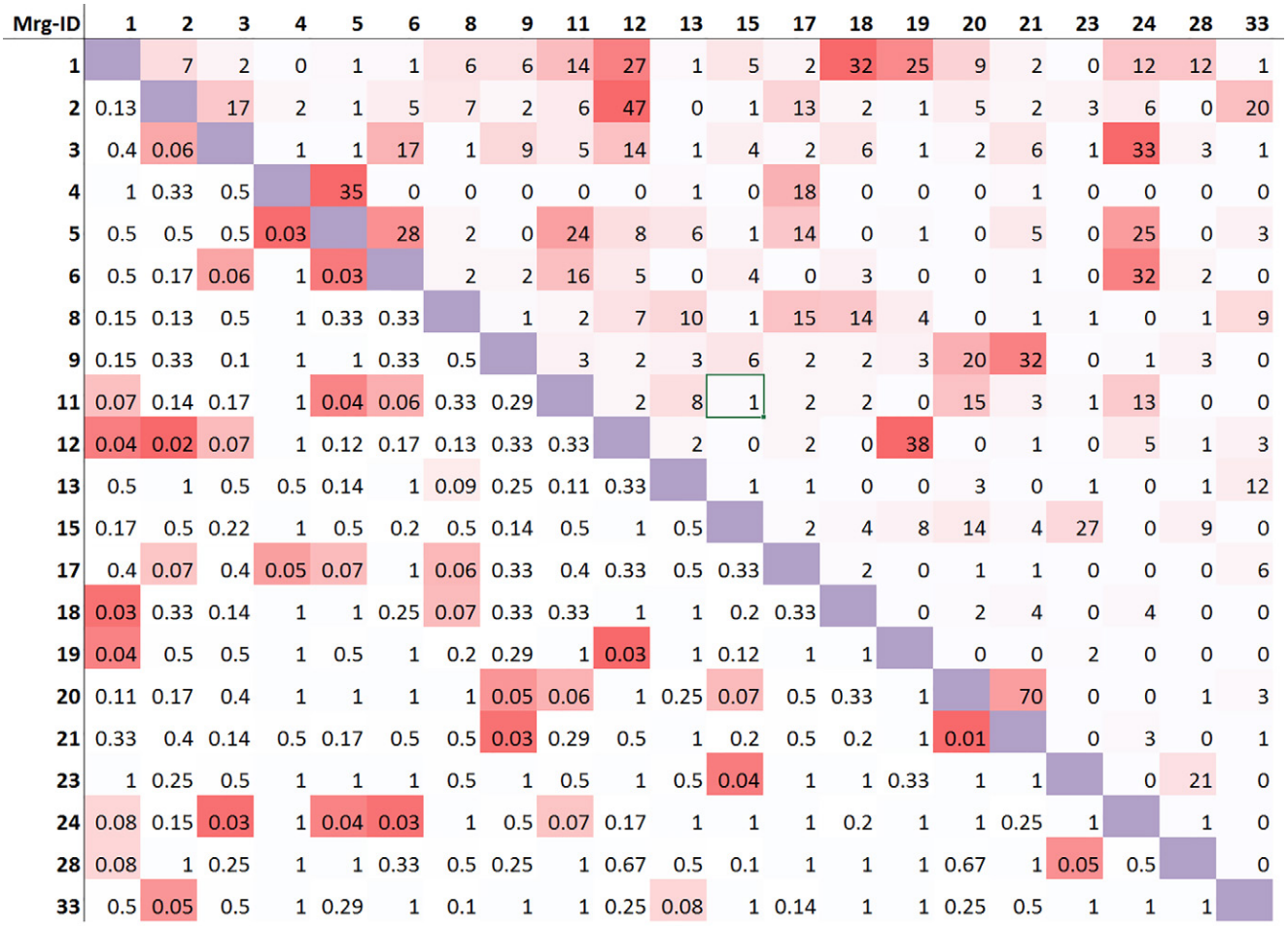

Mrg-ID	1	2	3	4	5	6	8	9	11	12	13	15	17	18	19	20	21	23	24	28	33
1		7	2	0	1	1	6	6	14	27	1	5	2	32	25	9	2	0	12	12	1
2	0.13		17	2	1	5	7	2	6	47	0	1	13	2	1	5	2	3	6	0	20
3	0.4	0.06		1	1	17	1	9	5	14	1	4	2	6	1	2	6	1	33	3	1
4	1	0.33	0.5		35	0	0	0	0	0	1	0	18	0	0	0	1	0	0	0	0
5	0.5	0.5	0.5	0.03		28	2	0	24	8	6	1	14	0	1	0	5	0	25	0	3
6	0.5	0.17	0.06	1	0.03		2	2	16	5	0	4	0	3	0	0	1	0	32	2	0
8	0.15	0.13	0.5	1	0.33	0.33		1	2	7	10	1	15	14	4	0	1	1	0	1	9
9	0.15	0.33	0.1	1	1	0.33	0.5		3	2	3	6	2	2	3	20	32	0	1	3	0
11	0.07	0.14	0.17	1	0.04	0.06	0.33	0.29		2	8	1	2	2	0	15	3	1	13	0	0
12	0.04	0.02	0.07	1	0.12	0.17	0.13	0.33	0.33		2	0	2	0	38	0	1	0	5	1	3
13	0.5	1	0.5	0.5	0.14	1	0.09	0.25	0.11	0.33		1	1	0	0	3	0	1	0	1	12
15	0.17	0.5	0.22	1	0.5	0.2	0.5	0.14	0.5	1	0.5		2	4	8	14	4	27	0	9	0
17	0.4	0.07	0.4	0.05	0.07	1	0.06	0.33	0.4	0.33	0.5	0.33		2	0	1	1	0	0	0	6
18	0.03	0.33	0.14	1	1	0.25	0.07	0.33	0.33	1	1	0.2	0.33		0	2	4	0	4	0	0
19	0.04	0.5	0.5	1	0.5	1	0.2	0.29	1	0.03	1	0.12	1	1		0	0	2	0	0	0
20	0.11	0.17	0.4	1	1	1	1	0.05	0.06	1	0.25	0.07	0.5	0.33	1		70	0	0	1	3
21	0.33	0.4	0.14	0.5	0.17	0.5	0.5	0.03	0.29	0.5	1	0.2	0.5	0.2	1	0.01		0	3	0	1
23	1	0.25	0.5	1	1	1	0.5	1	0.5	1	0.5	0.04	1	1	0.33	1	1		0	21	0
24	0.08	0.15	0.03	1	0.04	0.03	1	0.5	0.07	0.17	1	1	1	0.2	1	1	0.25	1		1	0
28	0.08	1	0.25	1	1	0.33	0.5	0.25	1	0.67	0.5	0.1	1	1	1	0.67	1	0.05	0.5		0
33	0.5	0.05	0.5	1	0.29	1	0.1	1	1	0.25	0.08	1	0.14	1	1	0.25	0.5	1	1	1	

Fig. 8. Heat map of similarity among oat consensus groups (numbered on axes). Cells above the diagonal show the total number of reciprocal BLASTn matches (*N*) between nonidentical markers on two given consensus groups at a threshold of $e \leq 10^{-20}$. Reciprocals of ($N + 1$), used for distance-based clustering, are shown below the diagonal. The strongest matches, indicating the likely homeology, are shown in gradients of red.

smaller and appear to suggest frequent rearrangements that diverge substantially from any patterns of original triplets. These results further confirm previous observations by Wight et al. (2003) and Gutierrez-Gonzalez and Garvin (2011) that the subgenomes within hexaploid oat are highly fragmented and restructured. These new results provide more detailed information about homeologous relationships, which will be essential in guiding future sequencing projects and reconciling the hexaploid genome with that of its diploid progenitors.

Because of these frequent subgenome rearrangements in oat, it will be important in future work to characterize regions of consistency further, as well as to document the exact positions of rearrangement events. Some rearrangements may be ancient and stable, whereas others may be recent, diverging among parents, including those used to produce this consensus map. From the combined analyses of alternate placement (Fig. 7) and homeolog matching (Fig. 8 and Fig. 9), we may be able to distinguish between stable homeologous relationships and those that are heterogeneous among mapping populations. Support for heterogeneous translocation events may be provided by pairs of chromosomes showing high rates of alternate placement but low sequence-based similarity. For example, Mrg 11 and Mrg 15 showed the highest levels of alternate placement (Fig. 7) but a very low level of sequence similarity among markers (Fig. 8). Further inspection of the detailed alternate placement between Mrg 11 and Mrg 15 (Supplemental Table S2) shows that this phenomenon involves markers throughout most of Mrg 15, but is unique to one end of Mrg 11. The fact that an alternate consensus (Mrg 11v) was found for Mrg 11 (see Supplemental Fig. S3) suggests that the populations AM, DE, and OT may contain a different configuration and/or translocation of this chromosome. This observation reinforces the need to examine individual populations in relation to the consensus map to determine if a gene or quantitative trait locus of interest may be located on a nonstandard chromosome configuration.

In contrast, one of the strongest pairs of matches in both types of analysis is between Mrg 20 and Mrg 21. These chromosomes correspond to groups previously designated KO_22_44_18 and KO_24_26_34 by Wight et al. (2003), who also identified them as homeologs. These chromosomes also contain the suspected location of homeologous versions of the vernalization-related

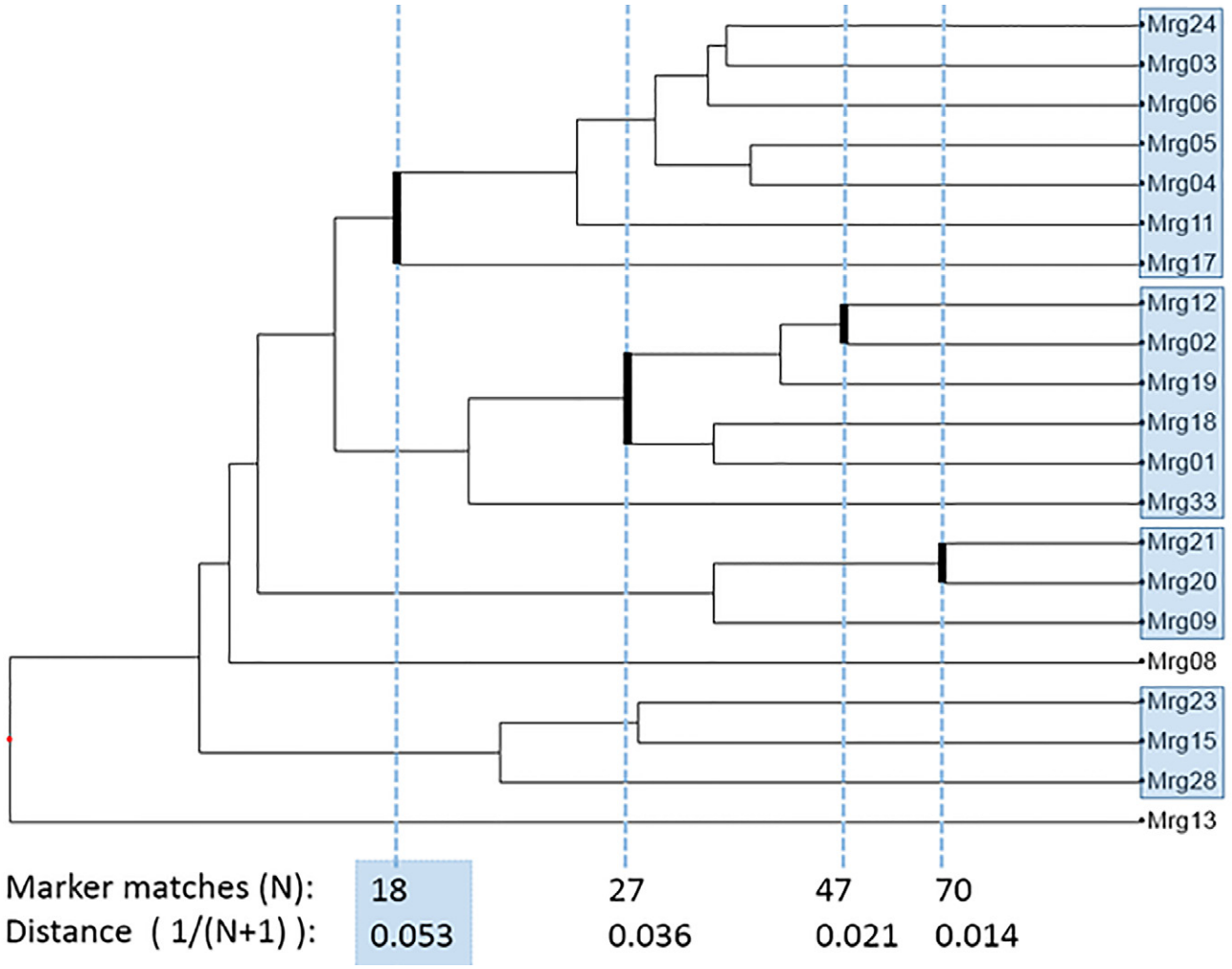

Fig. 9. Clusters of oat consensus chromosomes [Merge (Mrg) 01 through Mrg 33] formed by minimum distance joins using distances calculated as $(1 + N)^{-1}$, where N is the number of reciprocal BLASTn matches at $e \leq 10^{-20}$ between markers mapped or placed on alternate chromosome pairs. "Merge" indicates linkage groups that are the consensus of the underlying component maps. Distances and corresponding N values are shown at selected joins. Blue shading indicates clusters formed at $N \geq 18$.

Vrn1 locus (Nava et al., 2012). Although we do not have a confirmed physical assignment for these chromosomes, we suspect them to be a homeologous A–D pair. If this is the case, then one of the previous assignments of this pair of chromosomes to 19A and 16A (Oliver et al., 2013) must be incorrect.

Ortholog Matching and Synteny Inference

The availability of long expressed sequences from which the array-based markers were designed provided high-confidence sequence matches to many model genomes (data not shown), including excellent matches to the public rice genome, from which inferences were made regarding the most likely regions of synteny (Fig. 10). Sequence matches to GBS markers also contributed to this analysis but because these markers are based on short genomic reads, they provided fewer than 15% of the rice matches, despite being the majority of mapped markers. Although eight grass genome sequences have been published, a recent meta-analysis by Wang et al. (2015) provides convincing evidence that the rice genome has undergone the slowest nucleotide substitution rate and that it provides the best current approximation of the ancestral grass genome. For this reason, we have focused our comparative analysis on rice. We note, however, that comparison to other grasses or model organisms may be relevant for purposes of orthology-based cloning of genes for which rice is not the best model; for this purpose, the sequence data of the markers have been made available online.

Many of the inferences regarding rice synteny that are presented in Fig. 10 are similar to those presented in figure 4 of Oliver et al. (2013), particularly for those chromosomes where the oat map has not been revised. However, the current inferences should be considered more reliable for three reasons: first, there have been major and minor revisions of the consensus map (see Supplemental Fig. S4); second, the current analysis is based on a much larger number and higher density of markers; and third, the matches in Fig. 10 are scaled in cM, whereas those shown by Oliver et al. (2013) were based on one unit per marker and therefore were biased toward marker-dense regions. An example of an improved inference is

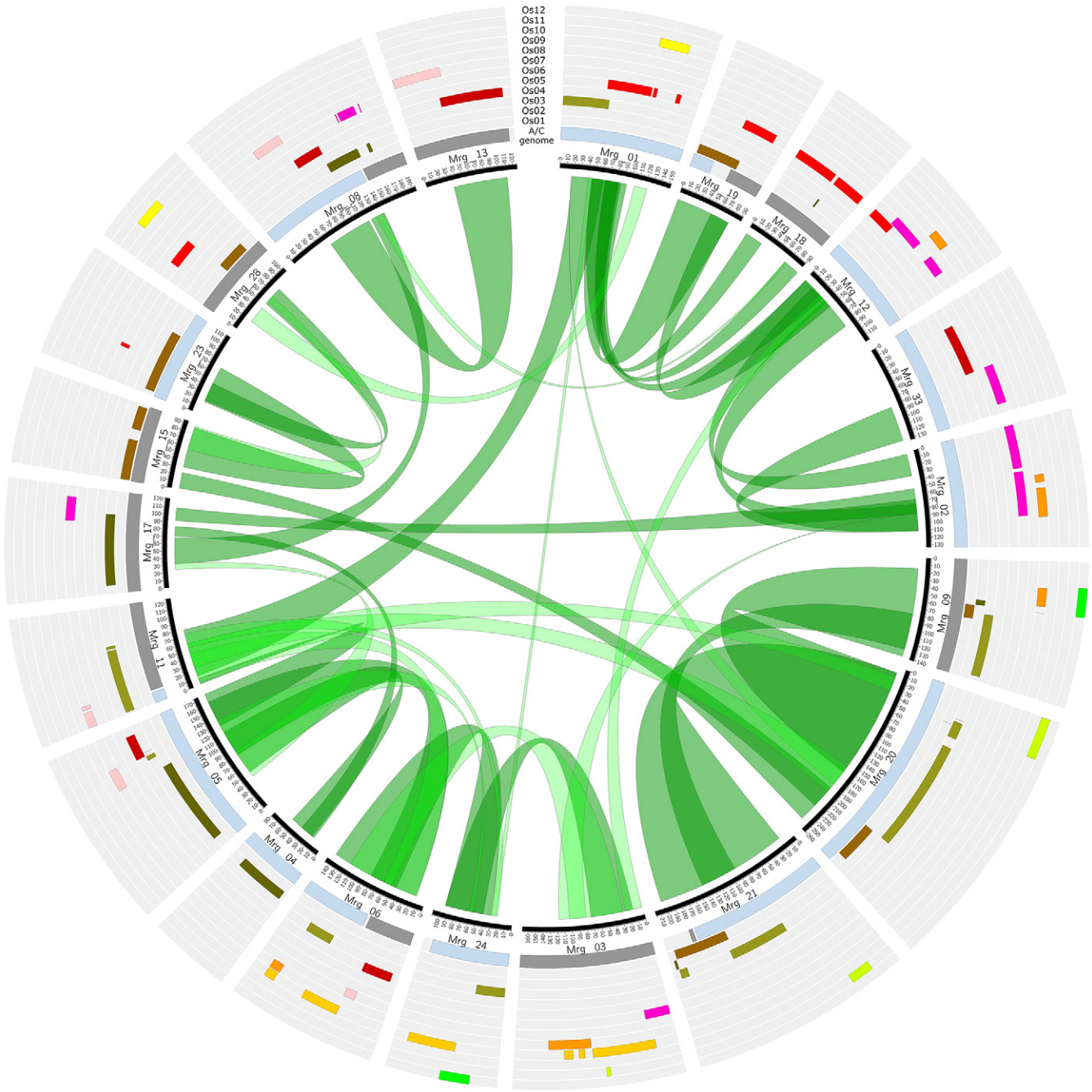

Fig. 10. Circle diagram showing 21 oat consensus chromosomes with cM units. Regions of inferred reciprocal homeology based on the chromosome with the greatest number of BLASTn matches ($e \leq 10^{-20}$) are indicated by green ribbons decorating the interior of the circle. The choice of dark green (strong match) versus light green (weaker match) was determined subjectively on the basis of the density of matches in the regions connected by ribbons. The first outer ring indicates regions that predominantly match shotgun sequence reads from an A-genome diploid oat (blue) or a C-genome diploid oat (gray). The 12 remaining multicolored outer rings indicate inferred regions of greatest orthology to one of the 12 rice chromosomes (*Os*01 through *Os*12) based on the highest number of tBLASx or BLASTn matches ($e \leq 10^{-20}$) within a sliding 30-cM window. For both the homeology and rice orthology, a second match is shown only when the evidence is within 20% of the best match.

the case of Mrg 21, formerly named 16A by Oliver et al. (2013). The new analysis shows that Mrg 21 has extensive orthologous regions to rice chromosomes 1 and 3, with a shorter region being similar to rice chromosome 11. This is almost exactly the same pattern of orthology seen with the highly homeologous Mrg 20. However, the region of orthology to rice chromosome 3 on the former 16A was not apparent in the earlier work; instead, a region similar to rice chromosome 2 was inferred. In this case, the discrepancy appears to be caused by a revision of the consensus map whereby Mrg 21 has been lengthened to include markers that were not formerly mapped and has lost a region formerly assigned to chromosome 16A, which is now incorporated into Mrg

05 (see Supplemental Fig. S4). The current revision and orthology assignment for this pair of chromosomes is more consistent with a parsimonious outcome of genome evolution and will aid substantially with any orthology-based inferences about these two chromosomes.

Although all rice chromosomes are represented in the new orthology matches to oat, some are represented in larger or more contiguous stretches than others. The most highly represented rice chromosomes appear to be those that match within the most conserved homeology clusters. These include the previously mentioned cluster of Mrg 20, Mrg 21, and Mrg 09 (matching rice chromosome 1 and 3), as well as Mrg 15, Mrg 23, and Mrg 28 (matching rice chromosome 1); Mrg 03, Mrg 06, and Mrg 24 (matching rice chromosome 9); and Mrg 04, Mrg 05, and Mrg 17 (matching rice chromosome 2). The oat chromosomes where homeology appears to be the most disrupted (e.g., Mrg 01 and Mrg 08) are also regions where the orthology matches are the shortest and least continuous. Nevertheless, segments where homeology is apparent (e.g., part of Mrg 01 and Mrg 11) usually contain a coinciding match to rice (in this case, rice chromosomes 3).

CONCLUSION

Developing an accurate and representative consensus linkage map in hexaploid oat has been a formidable challenge faced by the oat community for many years. The present work is the culmination of a collaborative effort to generate a dense map of sequence-based markers that incorporates information from many different populations. This work clarifies, beyond doubt, that there are heterogeneous physical chromosome rearrangements among adapted oat varieties that have complicated and will continue to complicate mapping efforts. Thus it is important that the research community understands that this consensus map is a rule from which exceptions are built. Regions where homeology and orthology are highly conserved are evident and these may provide the easiest models for further research; however, those regions where subgenome homeology is most disrupted may provide interesting avenues for further research into the dynamics of polyploid evolution. Such work will be aided by future genome sequencing efforts, including those focusing on diploid oat ancestors. Although, it is disappointing that the physical assignment of chromosomes could not be completed, as was intended by the experimental design, we feel that the current confirmed assignments are a good foundation for further work and that the community should proceed with a cautious multifaceted approach to the identification and validation of the remaining chromosome assignments. The substantial grass synteny, as illustrated by our comparisons to rice, is not a surprise to the grass genome research community. However, the ability to now pursue specific regions of conservation or rearrangement will accelerate orthology-based gene discovery in oat and may encourage new avenues of exploration into the evolutionary events that follow polyploidization.

Acknowledgments

ASC, Y-FH, and SS contributed equally as first authors; JAS and NAT contributed equally as senior corresponding authors. The authors acknowledge the generous support for this project provided to the Collaborative Oat Research Enterprise by General Mills, the North American Millers' Association, the Prairie Oat Growers' Association of Canada, USDA-NIFA, and Agriculture and Agri-food Canada. We are also grateful to the students and many sponsors of the Plant Pathways Elucidation Project (http://p2ep.org, accessed 9 Mar. 2016). We are indebted to many others, too numerous to mention, who provided excellent advice and technical support to the authors. Financial support to JAS was provided by National Science Foundation Award #1444575.

References

Babiker, E.M., T.C. Gordon, E.W. Jackson, S. Chao, S.A. Harrison, M.L. Carson, et al. 2015. Quantitative trait loci from two genotypes of oat (*Avena sativa*) conditioning resistance to *Puccinia coronata*. Phytopathology 105:239–245. doi:10.1094/PHYTO-04-14-0114-R

Baptista-Giacomelli, F., M. Pagliarini, and J. de Almeida. 2000. Chiasma frequency, distribution and terminalization in hexaploid oats (*Avena sativa* L.). Acta Sci. 22:269–273.

Close, T.J., P.R. Bhat, S. Lonardi, Y. Wu, N. Rostoks, L. Ramsay, et al. 2009. Development and implementation of high-throughput SNP genotyping in barley. BMC Genomics 10:582. doi:10.1186/1471-2164-10-582

FAO. 2013. FAOStat: Statistical Division of the Food and Agriculture Organization of the United Nations (2013 data). Food and Agricultural Organization of the United Nations. http://faostat.fao.org/. (accessed 27 Apr. 2016).

Foresman, B.J. 2014. Identification of quantitative trait loci and comparison of selection methods for barley yellow dwarf tolerance in spring oats and winter wheat. M.S. thesis, Univ. Illinois at Urbana-Champaign.

Fox, S.L., E.N. Jellen, S.F. Kianian, H.W. Rines, and R.L. Phillips. 2001. Assignment of RFLP linkage groups to chromosomes using monosomic F_1 analysis in hexaploid oat. Theor. Appl. Genet. 102:320–326. doi:10.1007/s001220051648

Gale, M.D., and K.M. Devos. 1998. Plant comparative genetics after 10 years. Science 282:656–659. doi:10.1126/science.282.5389.656

Gutierrez-Gonzalez, J.J., and D.F. Garvin. 2011. Reference genome-directed resolution of homologous and homeologous relationships within and between different oat linkage maps. Plant Gen. 4:178–190. doi:10.3835/plantgenome2011.01.0004

He, X., H. Skinnes, R.E. Oliver, E.W. Jackson, and Å. Bjørnstad. 2013. Linkage mapping and identification of QTL affecting deoxynivalenol (DON) content (*Fusarium* resistance) in oats (*Avena sativa* L.). Theor. Appl. Genet. 126:2655–2670. doi:10.1007/s00122-013-2163-0

Hizbai, B.T., K.M. Gardner, C.P. Wight, R.K. Dhanda, S.J. Molnar, D. Johnson, et al. 2012. Quantitative trait loci affecting oil content, oil composition, and other agronomically important traits in oat. Plant Gen. 5:164–175. doi:10.3835/plantgenome2012.07.0015

Jaccoud, D., D. Peng, D. Feinstein, and A. Kilian. 2001. Diversity arrays: A solid state technology for sequence information independent genotyping. Nuc. Acids Res. 29:e25. doi:10.1093/nar/29.4.e25.

Jellen, E., and J. Beard. 2000. Geographical distribution of a chromosome 7C and 17 intergenomic translocation in cultivated oat. Crop Sci. 40:256–263. doi:10.2135/cropsci2000.401256x

Jellen, E., B. Gill, and T. Cox. 1994. Genomic in situ hybridization differentiates between A/D-and C-genome chromatin and detects intergenomic translocations in polyploid oat species (genus *Avena*). Genome 37:613–618. doi:10.1139/g94-087

Jellen, E.N., H.W. Rines, S.L. Fox, D.W. Davis, R.L. Phillips, and B.S. Gill. 1997. Characterization of 'Sun II' oat monosomics through C-banding and identification of eight new 'Sun II'monosomics. Theor. Appl. Genet. 95:1190–1195. doi:10.1007/s001220050680

Klos, K.E., Y.-F. Huang, W.A. Bekele, D.E. Obert, E. Babiker, A.D. Beattie, et al. 2016. Population genomics related to adaptation in elite oat germplasm. Plant Gen. doi:10.3835/plantgenome2015.11.0113 (in press)

Kremer, C., M. Lee, and J. Holland. 2001. A restriction fragment length polymorphism based linkage map of a diploid *Avena* recombinant inbred line population. Genome 44:192–204. doi:10.1139/gen-44-2-192

Krzywinski, M., J. Schein, I. Birol, J. Connors, R. Gascoyne, D. Horsman, et al. 2009. Circos: An information aesthetic for comparative genomics. Genome Res. 19:1639–1645. doi:10.1101/gr.092759.109

Lin, Y., B.N. Gnanesh, J. Chong, G. Chen, A.D. Beattie, J.W. Mitchell Fetch, et al. 2014. A major quantitative trait locus conferring adult plant partial resistance to crown rust in oat. BMC Plant Biol. 14:250. doi:10.1186/s12870-014-0250-2

McCartney, C.A., R.G. Stonehouse, B.G. Rossnagel, P.E. Eckstein, G.J. Scoles, T. Zatorski, et al. 2011. Mapping of the oat crown rust resistance gene *Pc91*. Theor. Appl. Genet. 122:317–325. doi:10.1007/s00122-010-1448-9

Muñoz-Amatriaín, M., M.J. Moscou, P.R. Bhat, J.T. Svensson, J. Bartoš, P. Suchánková, et al. 2011. An improved consensus linkage map of barley based on flow-sorted chromosomes and single nucleotide polymorphism markers. Plant Gen. 4:238–249. doi:10.3835/plantgenome2011.08.0023

Nava, I.C., C.P. Wight, M.T. Pacheco, L.C. Federizzi, and N.A. Tinker. 2012. Tagging and mapping candidate loci for vernalization and flower initiation in hexaploid oat. Mol. Breed. 30:1295–1312. doi:10.1007/s11032-012-9715-x

O'Donoughue, L.S., M.E. Sorrells, S.D. Tanksley, E. Autrique, A.V. Deynze, S.F. Kianian, et al. 1995. A molecular linkage map of cultivated oat. Genome 38:368–380. doi:10.1139/g95-048

O'Donoughue, L.S., Z. Wang, M. Röder, B. Kneen, M. Leggett, M.E. Sorrells, et al. 1992. An RFLP-based linkage map of oats based on a cross between two diploid taxa (*Avena atlantica* × *A. hirtula*). Genome 35:765–771. doi:10.1139/g92-117

Oliver, R.E., N.A. Tinker, G.R. Lazo, S. Chao, E.N. Jellen, M.L. Carson, et al. 2013. SNP discovery and chromosome anchoring provide the first physically-anchored hexaploid oat map and reveal synteny with model species. PLoS ONE 8:E58068. doi:10.1371/journal.pone.0058068

Pallotta, M.A., P. Warner, R.L. Fox, H. Kuchel, S.J. Jefferies, and P. Langridge. 2003. Marker assisted wheat breeding in the southern region of Australia. In: N.E. Pogna and R.A. McIntosh, editors, Proceedings of the 10th International Wheat Genetics Symposium, Paestum, Italy. 1–6 Sept. 2003.. Istituto Sperimentale per la Cerealicoltura, Fiorenzuola d'Arda, Italy. p. 1–6

Portyanko, V.A., D.L. Hoffman, M. Lee, and J.B. Holland. 2001. A linkage map of hexaploid oat based on grass anchor DNA clones and its relationship to other oat maps. Genome 44:249–265. doi:10.1139/g01-003

Rooney, R.L., H.W. Rines, and R.L. Phillips. 1994. Markers linked to crown rust resistance genes *Pc 91* and *Pc* in oat. Crop Sci. 34:940–944. doi:10.2135/cropsci1994.0011183X003400040019x

Sanz, M.J., E.N. Jellen, Y. Loarce, M.L. Irigoyen, E. Ferrer, and A. Fominaya. 2010. A new chromosome nomenclature system for oat (*Avena sativa* L. and *A. byzantina* C. Koch) based on FISH analysis of monosomic lines. Theor. Appl. Genet. 121:1541–1552. doi:10.1007/s00122-010-1409-3

Tinker, N.A. 2010. SPAGHETTI: Simulation software to test genetic mapping programs. J. Hered. 101:257–259. doi:10.1093/jhered/esp109

Tinker, N.A., S. Chao, G.R. Lazo, R.E. Oliver, Y.-F. Huang, J.A. Poland, et al. 2014. A SNP genotyping array for hexaploid oat. Plant Genome 7(3): doi:10.3835/plantgenome2014.03.0010

Tinker, N.A., A. Kilian, C.P. Wight, K. Heller-Uszynska, P. Wenzl, H.W. Rines, et al. 2009. New DArT markers for oat provide enhanced map coverage and global germplasm characterization. BMC Genomics 10:39. doi:10.1186/1471-2164-10-39

Wang, S., D. Wong, K. Forrest, A. Allen, S. Chao, B.E. Huang, et al. 2014. Characterization of polyploid wheat genomic diversity using a high-density 90,000 single nucleotide polymorphism array. Plant Biotechnol. J. 12:787–796. doi:10.1111/pbi.12183

Wang, X., J. Wang, D. Jin, H. Guo, T.H. Lee, T. Liu, and A.H. Paterson. 2015. Genome alignment spanning major Poaceae lineages reveals heterogeneous evolutionary rates and alters inferred dates for key evolutionary events. Mol. Plant 8:885–898. doi:10.1016/j.molp.2015.04.004

Wight, C.P., L.S. O'Donoughue, J. Chong, N.A. Tinker, and S.J. Molnar. 2004. Discovery, localization, and sequence characterization of molecular markers for the crown rust resistance genes *Pc38*, *Pc39*, and *Pc48* in cultivated oat (*Avena sativa* L.). Mol. Breed. 14:349–361. doi:10.1007/s11032-004-0148-z

Wight, C.P., N.A. Tinker, S.F. Kianian, M.E. Sorrells, L.S. O'Donoughue, D.L. Hoffman et al. 2003. A molecular marker map in 'Kanota' × 'Ogle' hexaploid oat (*Avena* spp.) enhanced by additional markers and a robust framework. Genome 46:28–47. doi:10.1139/g02-099

Wu, Y., P.R. Bhat, T.J. Close, and S. Lonardi. 2008. Efficient and accurate construction of genetic linkage maps from the minimum spanning tree of a graph. PLoS Genet. 4:E1000212. doi:10.1371/journal.pgen.1000212

Yan, H., S.L. Martin, W.A. Bekele, R.G. Latta, A. Diederichsen, Y. Peng, et al. 2016. Genome size variation in the genus *Avena*. Genome (in press).